Index

1. Abbreviations 3
2. Abstract 4
3. Introduction 5
   - 3.1 What is Malignant Pleural Mesothelioma 5
   - 3.2 Asbestos and tumorigenicity 5
   - 3.3 Diagnosis and histologic characterization of MPM 8
   - 3.4 Genetics of MPM 11
   - 3.5 Current treatments for MPM 13
   - 3.6 High throughput screenings for drug repurposing 21
4. Aims 22
   - 4.1 AIM1 – Investigating the role of macrophages in response to asbestos 23
   - 4.2 AIM2 – Investigating the role of autophagy in tumour initiation 23
   - 4.3 AIM3 – Investigating the role of autophagy and BCL-X_L in drug resistance 23
   - 4.4 AIM4 – Using high throughput screenings to identify drugs synergic with current chemotherapy 23
   - 4.5 AIM5 – Validation of drug repurposing screening *in vitro* 23
5. Materials and methotds 23
   - 5.1 Cell lines and cell culture 23
   - 5.2 Nuclear staining and nuclei count. 24
   - 5.3 THP-1-derived macrophages differentiation and polarization. 25
   - 5.4 Crocidolite fibers handling and cell treatment 26
   - 5.5 RNA extraction, DNase treatment, and reverse transcription. 27
   - 5.6 Real-Time Polymerase Chain Reaction (RT-PCR). 28
   - 5.7 Conditioning of mesothelial cells with macrophage supernatants. 28
   - 5.8 Western blot (WB) 29
   - 5.9 Transfection of Met5A cells with LC3-eGFP-mRFP reporter. 30
   - 5.10 LC3-eGFP-mRFP reporter detection. 31
   - 5.11 Luciferase detection. 32
   - 5.12 Sigle clone selection with limit dilution method. 32
   - 5.13 Resazurin-based cell viability assay. 32
   - 5.14 High throughput screening for drug repurposing. 32
   - 5.15 Secondary screening and hit validation 33
   - 5.16 Synergy evaluation with Combenefit. 34
   - 5.17 Primary mesothelioma cells isolation. 34
   - 5.18 Evaluation of markers' expression upon combination treatment. 36

5.19 Spheroids formation and treatment. 36
5.20 Spheroid size analysis. 37
5.21 Statistical analysis. 39
6. Results 41
6.1 AIM1 – Investigating the role of macrophages in response to asbestos. 41
6.2 AIM2 – Investigating the role of autophagy in tumour initiation. 42
6.3 AIM3 – Investigating the role of autophagy and BCL-XL in drug resistance. 45
6.4 AIM4 – Using high throughput screenings to identify drugs synergic with current chemotherapy. 46
6.5 AIM5 – Validation of drug repurposing screening *in vitro.* 53
7. Discussion 66
8. References 73

1. Abbreviations

ABCB1 – ATP Binding Cassette B1

ABCG2 – ATP Binding Cassette G2

APC – Antigen-Presenting Cells

BAP1 – BRCA-associated protein 1

CDK4/6 – Cyclin-Dependent Kinase 4/6

CDKN2A – Cyclin Dependent Kinase Inhibitor 2A

CMV – Cytomegalovirus

CT – Computerized Tomography

CTLA-4 – Cytotoxic T Lymphocyte Antigen-4

DMSO – Dimethyl sulfoxide

EBUS – Endobronchial Ultrasound

EC_{50} – Effective Concentration 50%

EHZ2 – Enhancer of Zeste Homolog 2

EMA – European Medicines Agency

EPP – Extrapleural Pneumonectomy

FAD – Flavine Adenine Dinucleotide

FDA – Food and Drug Administration

FL – Firefly Luciferase

FMN – Flavine Mononucleotide

GABA – Gamma-Aminobutyric Acid

GFP – Green Fluorescent Protein

HESFM – Human Endothelial Serum Free Medium

HTS – High Throughput Screening

IHC – Immunohistochemistry

MDM2 – Murine Double Minute 2

MERLIN – Moesin-Ezrin-Radixin Like

MHC – Major Histocompatibility Complex

MPM – Malignant Pleural Mesothelioma

MRI – Magnetic Resonance Imaging

NF2 – Neurofibromin 2

o/n – Overnight

P/D – Pleurectomy/Decortication

PD1 – Programmed cell Death-1

PD-L1 – Programmed cell Death Ligand-1

PD-L2 – Programmed cell Death Ligand-2

PET – Positron Emission Tomography

PMA – Phorbol Myristate Acetate

PRC1 – Polycomb Repressive Complex 1

PRC2 – Polycomb Repressive Complex 2

RB – Retinoblastoma

RFP – Red Fluorescent Protein

ROS – Reactive Oxygen Species

RPMI – Roswell Park Memorial Institute Medium

RT-PCR – Real-Time Polymerase Chain Reaction

SMART – Surgery for Mesothelioma After Radiation Therapy

TAM – Tumour-Associated Macrophage

TCR – T Cell Receptor

TERT – Telomerase Reverse Transcriptase

WB – Western Blot

WT-1 – Wilms' tumour-1

2. Abstract

Malignant pleural mesothelioma (MPM) is a rare, aggressive malignancy affecting the pleura, the membrane lining the lungs, with a very poor prognosis. The current standard of care, besides surgery and/or radiotherapy in localised disease, is treatment with the chemotherapeutic agent cisplatin and pemetrexed, although their effectiveness remains limited, and they often leave space for the reoccurrence of chemotherapy-resistant mesothelioma. In this context, discovering treatments that can be substituted to chemotherapy or can effectively be combined with it is of utmost importance. In this project, 1520 FDA and EMA approved drugs were screened on the NCI-H28 mesothelioma cell line in vitro for their efficacy in killing tumour cells when used in combination with cisplatin. The best performing drugs (Riboflavin, Proglumide, Aminosalicylic acid, Gabapentin, Terfenadine, Propafenone, Oseltamivir) were further validated in vitro on two different mesothelioma cell lines to confirm their effectiveness and an attempt to understand their mechanism of action was made. In particular, the expression of CD24, OCT4 (cancer stem cell markers), ABCB1, ABCG2 (drug resistance markers), p21 (senescence marker), and BCL-XL (autophagy and apoptosis regulator) was analyzed upon treatment with the chosen drugs. No substantial difference in the expression of these markers between cells treated with cisplatin alone and cells treated with cisplatin plus each drug was observed, suggesting that other mechanisms are at play and further investigations are needed. Nonetheless, synergism was confirmed and scored by analysis with Lowe's algorithm. The efficacy of the selected drugs was also tested on primary mesothelioma cells isolated from patients undergoing biopsies or surgery and treated with the different drugs combined with cisplatin. Interestingly, cells isolated from different patients showed sensitivity to different drugs. Furthermore, to validate the drug combinations' effectiveness in a three-dimensional setting, mesothelioma spheroids were produced, and their size was evaluated upon treatment with the drugs combination. To conclude the project, evaluating the safety and effectiveness of the drugs combinations in an in vivo setting will be crucial. Therefore, an in vivo xenograft mouse model will be used to evaluate tumour size in untreated mice, cisplatin-treated mice, and mice treated with a combination of cisplatin and selected drugs.

3. Introduction

3.1 What is Malignant Pleural Mesothelioma

Malignant pleural mesothelioma (MPM, Figure 1) is the most common primary tumour of the pleura, and it is associated with asbestos exposure in over 80% of cases [5], where inhaled asbestos fibers move to the lung parenchyma and then to the pleura. There, they promote MPM onset [6, 7]. Interestingly, the tumour arises decades after exposure to asbestos, which poses some difficulties to the study of this tumour, especially its onset mechanisms. Although this tumour is rare, its incidence is increasing worldwide because asbestos has not been universally banned yet. Unfortunately, MPM is also a tumour with a very poor prognosis, with a 5-year survival rate of 24% for localised disease and of 7% for metastatic disease [8].

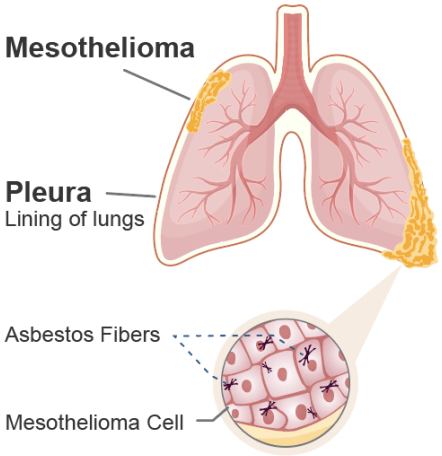

***Figure 1- graphic illustration of pleural mesothelioma**. Adapted from https://www.mesotheliomahope.com/mesothelioma/*

3.2 Asbestos and tumorigenicity

Asbestos is a naturally occurring silicate mineral. It is a very fibrous and brittle mineral that has been extensively exploited in the last few decades in various fields, especially construction, for its insulating and fire-resistant properties. Since the discovery of the carcinogenicity of asbestos, the use, commerce, elaboration, and extraction of this mineral has been forbidden in Europe, Australia, and U.S.A. Unfortunately, other countries are still extracting and using asbestos today, such as Russia, Kazakhstan, Brazil, India, China, and other South American and Asian countries [9].

***Figure 2 – Crocidolite** Adapted from Mineralogisches Museum Bonn (7385); "© Raimond Spekking / CC BY-SA 4.0.*

Although the term “asbestos” is commonly used for this type of mineral, two different categories can be distinguished based on their physical properties and chemical composition: serpentines and amphiboles. The former includes only chrysotile asbestos, which has curly fibers, and the latter is

further divided in five subclasses with straight fibers of different thickness and length, namely crocidolite (Figure 2), amosite, anthophyllite, tremolite, and actinolite.

All these types of asbestos differ in the shape and dimensions of their fibers, and this impacts on their ability to reach the more distal parts of the lungs, the alveoli, once inhaled. Their different chemical composition may also impact on the way these fibers interact with the cells present in their site of deposition [6].

When asbestos fibers are inhaled, they can reach and deposit in the lung alveoli. This is true especially for the straightest and smallest fibers. Then, it is verry difficult to clear the alveoli from the deposited fibers, and different fiber-cell interactions and cellular mechanisms are activated, beginning to set the environment for tumour onset [10].

Asbestos fibers are, in fact, not only responsible for the insurgence of pleural mesothelioma, but also lung adenocarcinoma , since their first and primary sites of deposition are lung alveoli, where they come in contact with alveolar epithelial cells [11].

From the alveoli, the fibers travel through the lymphatics and reach the pleura, where they can get stuck as a secondary deposition site. There they directly interact with resident macrophages and the mesothelial cells that constitute the visceral and parietal pleura [6] (Figure 3).

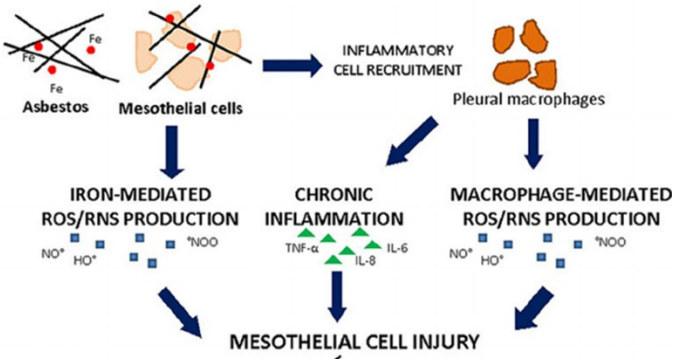

Figure 3 – schematic representation of mesothelioma onset, the action of asbestos fibers on macrophages and mesothelial cells *(https://www.researchgate.net/figure/Asbestos-induced-cell-injury-leading-to-mesothelioma-Mesothelial-cells-exposed-to-iron_fig2_278732107)*

Macrophages are in charge of phagocyting pathogens and foreign objects to clear them from the tissues. Asbestos fibers are no exception to this rule, but despite macrophages' attempts to phagocyte them, these cells are usually unable to completely engulf and digest them. This results in an aberrant process called *frustrated phagocytosis*, where macrophages produce high amounts of Reactive Oxygen Species (ROS) and secrete various cytokines that trigger inflammation. This process of frustrated phagocytosis persists for decades in the sites of fibers deposition, causing a local state of chronic inflammation considered to be one of the main drivers of mesothelioma onset [12-14].

The interaction of asbestos fibers with mesothelial cells is different in nature from that with macrophages. Asbestos fibers are, in fact, toxic for pleural mesothelial cells due to the DNA damage they cause to these cells [15]. This toxicity triggers, as well as an increased ROS production as for macrophages, the asbestos-induced death of mesothelial cells, and, in response, these cells activate cellular responses that enable them to survive. In particular, autophagy is thought to be the mechanism exploited by mesothelial cells to escape asbestos-induced cell death.

Autophagy can be either constitutive or induced, where constitutive autophagy recycles cellular components from aged or damaged organelles, while induced autophagy occurs in response to environmental challenges and protects cells from apoptosis and necrosis[16] [17] [18] . The autophagy flux is initiated by mTOR inhibition [19], which leads to the activation of Beclin 1 [19] and subsequent autophagy-related proteins (ATGs) recruitment and LC3 modification from LC3-I to LC3-II and insertion into the membrane of the autophagosome. In parallel, p62 cargo protein takes autophagic substances for degradation to the autophagosome. At a later stage of autophagy, autophagosomes fuse with lysosomes to become the autolysosome, where the contents of autophagosome are digested [19]. The levels of LC3-II and p62 can be used to assess autophagy and to distinguish autophagy induction. Autophagy allows a few mesothelial cells to survive despite accumulating DNA damage, thus increasing the chance of malignant transformation in these cells [15]. In particular, it has been shown that inhibiting activators of the autophagy pathway in mesothelial cells exposed to asbestos fibers leads to a decreased number of mesothelial cells able to form new clonal colonies (colony formation assay), thus reinforcing the hypothesis that the protective effect toward asbestos damage exerted by autophagy actually turns out to promote tumour development [15]. Interestingly, the concept of “apoptosis-primed cells” has been introduced by Xu *et al.,* since mesothelioma cells are expressing pro-apoptotic factors, but their apoptosis seems to be hampered by an overexpression the anti-apoptotic protein BCL-X_L and by an increase in autophagic activity compared to non-transformed mesothelial cells [20].

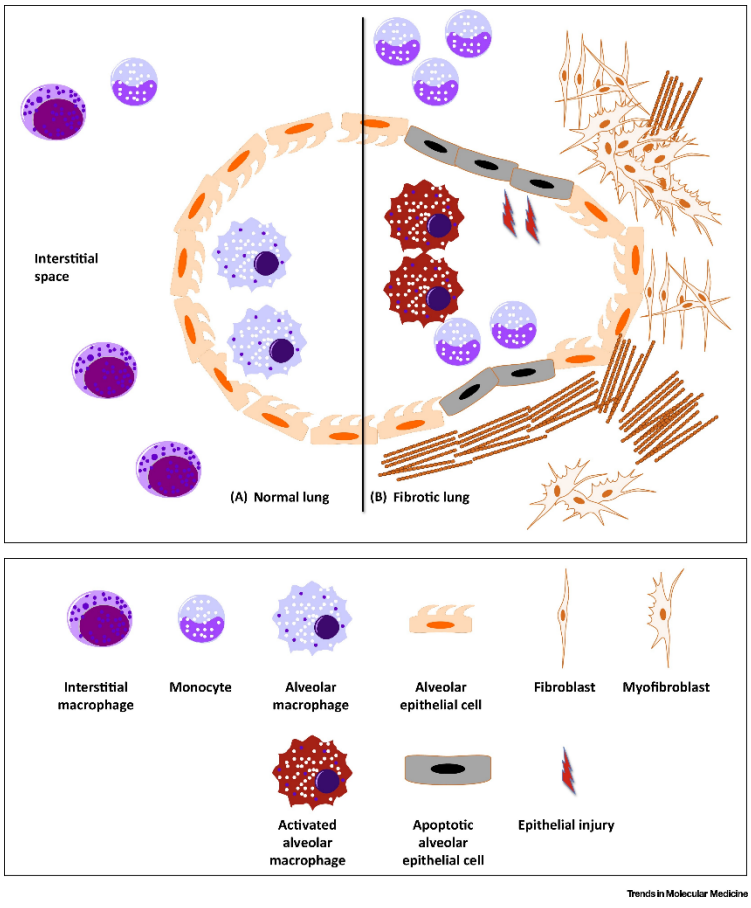

Figure 4 – schematic representation of the mechanism of asbestos-driven fibrosis onset in asbestosis. *Adapted from [1].*

It is important to note that tumour onset is not the only possible outcome of asbestos exposure. Asbestos fibers, being a damaging agent that usually cannot be cleared from the tissues, are often isolated from the tissues by being surrounded by fibrotic tissues. This process is usually led by macrophages, which secrete factors that induce fibroblasts to form a protective "scar" around the fibers. These small scarifications containing asbestos fibers are called *inclusion bodies* or *asbestos bodies* [21]. The asbestos bodies may be able to contain the damaging effects of asbestos fibers, but when they fail, the outcomes can be either the insurgence of the tumour or an aberrant scarring process that leads to the fibrosing of the lungs, called asbestosis [1]; Figure 4), or to the formation of fibrotic plaques in the pleura.

Shedding further light on the molecular mechanisms involved in malignant transformation in mesothelial cells is very important because it could open the way for the development of chemoprevention therapies aimed at preventing asbestos-induced mesothelioma onset in exposed individuals, which could reduce the incidence of this tumour.

3.3 Diagnosis and histologic characterization of MPM

The incidence of MPM is higher in males due to the difference in occupational exposure. It is a rare tumour with an average incidence of 0.7/100 000 people, although the incidence is higher in countries that used more asbestos in the last few decades, such as the Netherlands, UK, and Australia [22]. Furthermore, the incidence is currently still arising in other countries since mesothelioma appears around 40 years after asbestos exposure and in some parts of the world

asbestos is still extracted and used [9, 23]. Because of this, it is very rare for MPM to manifest in people younger than 50 years old, and the median age at diagnosis is over 70 years [24].

Usually patients present dyspnoea, cough, chest pain, and also weight loss. Also, unilateral pleural effusions are quite typical. Collecting the occupational history of the patient is of utmost importance to assess the eventual exposure to asbestos.

The diagnosis is done at first by chest radiography, which typically shows pleural thickening and effusion. This is not sensitive and specific enough to grant an unequivocal diagnosis and must be complemented by a computerised tomography (CT) of the chest with contrast medium, to be extended to the abdomen if the suspect of MPM is confirmed. In case the radiology suggests mesothelioma, a percutaneous thoracentesis can both reduce symptoms and allow a cytological diagnosis of malignant mesothelioma cells. Cytology can give false negatives, so it is also advised to perform a thoracoscopy and collect a biopsy to confirm the diagnosis by histology and immunohistochemistry [25]. CT scans and/or ultrasound-guided biopsies can be performed in case thoracoscopy is contraindicated or unfeasible for a specific patient. A positron emission tomography (PET) scan is sometimes performed to better ascertain the extension of the disease when surgery is planned. Other exams less frequently required are a magnetic resonance imaging (MRI), endobronchial ultrasound (EBUS), mediastinoscopy [25].

Up to date there are only a few potential circulating tumour markers that could help diagnosing MPM, but are not highly specific for this tumour, such as mesothelin. Therefore, their presence as circulating tumour markers must be considered very carefully and is not yet widely used in clinical practice [26].

When the malignancy is suspected to be a mesothelioma, characterization of the tumour is needed. A first classification of the tumour is done based on its histological features. In fact, MPM can be classified into three different histologic types: epithelioid, sarcomatoid, and biphasic (Figure 5) [27] [2].

Epithelioid mesothelioma is usually composed of round, epithelial-like cells, and usually has a cohesive architecture. It is the most represented type of mesothelioma and the one with the better prognosis.

Sarcomatoid mesothelioma is usually composed of elongated and spindle cells arranged in solid sheets or within a fibrous stroma. It is the rarest type and the one with the worst prognosis.

Biphasic mesothelioma has both epithelioid and sarcomatoid components in variable percentages, but each representing at least 10% of the tumour [27].

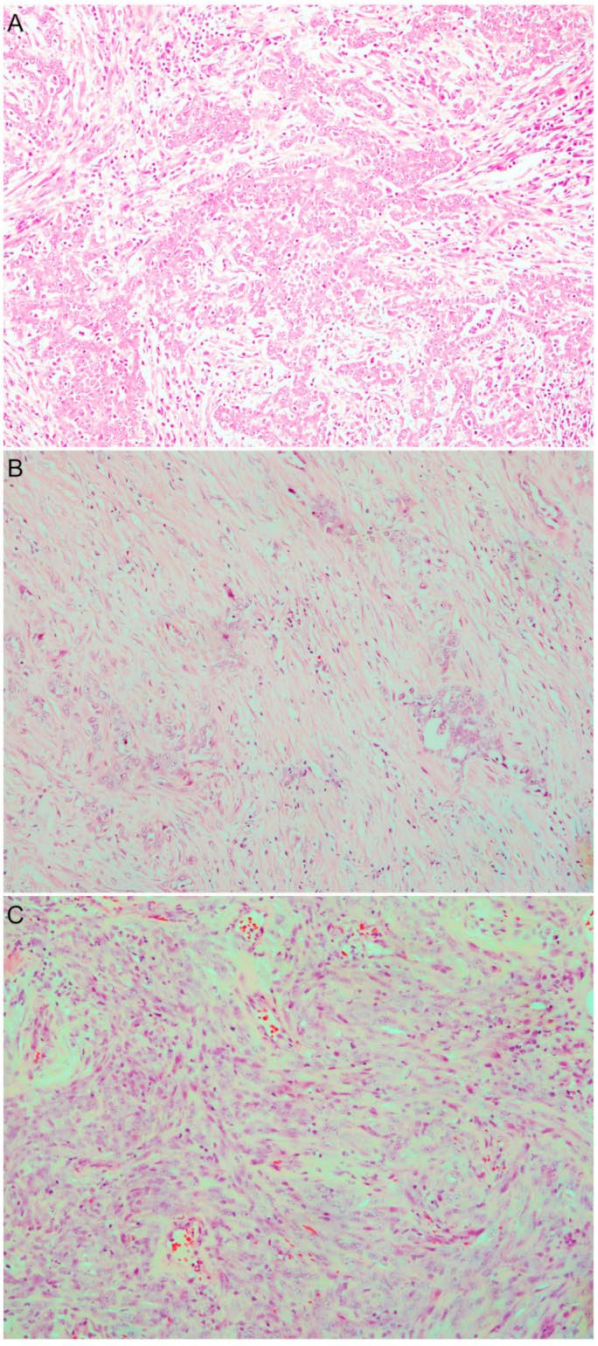

***Figure 5 – Representative pictures of the three histologic types of mesothelioma**. Epithelioid (A), biphasic (B), and sarcomatoid (C) mesothelioma. Image by Bruno et al. [2]*

Since the pleura is a common site for other metastatic diseases, recognising malignancies in the pleura as mesothelioma based on histology alone can be very problematic. For this reason, the use of immunohistochemistry (IHC) is required for the proper characterization of the tumour. In particular, it is advised to stain the biopsies for at least two mesothelioma-associated markers, such as calretinin, Wilms' tumour-1 (WT-1), and cytokeratin 5/6 to confirm the pleural origin of the tumour, and two adenocarcinoma-associated markers, such as CEA, Ber-EP4, and MOC-3 to rule out other malignancies [24]. While the analysis of these markers may be sufficient to properly diagnose epithelial mesotheliomas, staining for broad-spectrum cytokeratins may help the diagnosis of sarcomatoid mesothelioma and also to rule out sarcomas [24].

After the diagnosis, it is necessary to stage the tumour in order to proceed with the better course of action for treatment. The TNM system is the most widely used cancer staging system.

The T refers to the size of the primary tumour and the staging can range from T0, where the main tumour cannot be found, to T4, where a higher number indicates a bigger size of the primary tumour. TX means that the primary tumour's size cannot be measured.

The N refers to the number of nearby lymph nodes where the cancer has metastasized. It can range from N0, where the cancer has not spread to the nearby lymph nodes, to N3, where increasing number indicate a higher number of affected lymph nodes. NX means that the presence of cancer in the regional lymph nodes cannot be assessed.

The M refers to the presence of metastases. M0 means that the cancer has not metastasized, M1 means that the cancer has spread to other parts of the body, while MX means that the presence of metastases cannot be assessed [28].

Staging can be described more synthetically with a simpler system, derived from the grouping of TNM classes, where stage 0 means that abnormal cells are present, but they have not spread to the nearby tissue (Cancer In Situ), and stages I to III mean that the tumour has grown and it has spread in the nearby tissues, a higher number indicating a bigger growth and expansion. Stage IV is indicative of metastases to distant organs [28]. A "clinical stage" is attributed to the disease by means of imaging studies like CT and PET scans , while a "pathological stage" can be defined after surgery by means of the histological exam.

3.4 Genetics of MPM

While the histologic features and staging of mesothelioma are extremely important, the characterization of the genetic alterations of the tumour is of utmost importance, since they hold prognostic value and can represent a target for therapy.

The most frequently mutated gene in MPM is Cyclin Dependent Kinase Inhibitor 2A (*CDKN2A*) (37% overall in cBioPortal database, http://cbioportal.org), which usually presents deep deletions and, more rarely, other loss-of function mutations. *CDKN2A* is a tumour suppressor gene that encodes for two proteins, p16INK4a and p14ARF (Figure 6) {Ruas, 1998 #29} {Nag, 2013 #30}. p16INK4A has a key role in cell cycle regulation by inhibiting the Cyclin-Dependent Kinase 4/6 (CDK4/6)/Cyclin D1 complex, which in turn inhibits the antiproliferative activity of the retinoblastoma protein (RB). Therefore, the loss of p16INK4A leads to uncontrolled cell proliferation. The other product of gene *CDKN2A*, p14ARF, also affects the cell cycle by inhibiting the Murine Double Minute 2 (MDM2) protein, which is the principal inhibitor of p53 and promotes its ubiquitination and degradation. p14ARF-mediated inhibition of MDM2 therefore prevents the degradation of p53, that can exert its controlling function in cell cycle progression, e.g., in response to genotoxic damage [29, 30].

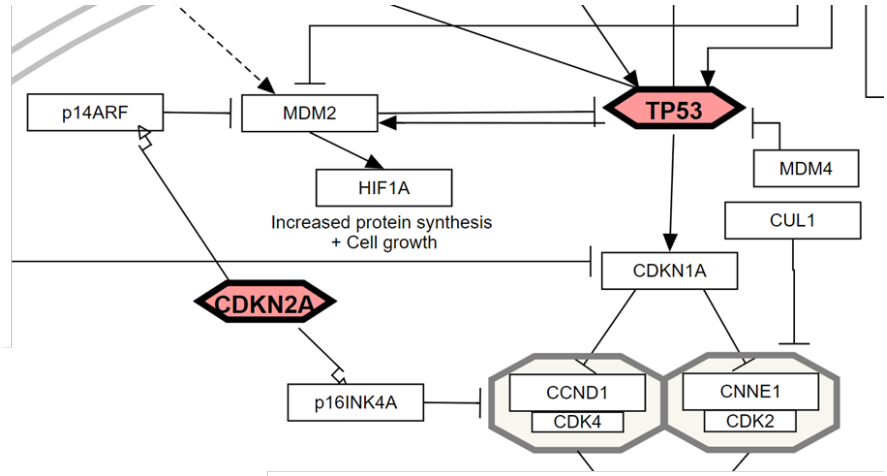

***Figure 6 – Close up pf CDKN2A role in mesothelioma pathways**. Adapted from [31].*

The second most frequently mutated gene in MPM is BRCA-associated protein 1 (*BAP1*) (31% overall in cBioPortal database, http://cbioportal.org), which is often burdened by loss of function mutations or presents deep deletions. The inactivation of BAP1 leads to increased expression of enhancer of zeste homolog 2 (*EZH2*), an epigenetic regulator involved in the activity of Polycomb repressive complexes 1 and 2 (PRC1 and PCR2) [32] (Figure 7). PRC1 and PRC2 have the key role of compacting chromatin, regulating important gene expression patterns. Therefore, their dysregulation due to BAP1 dysfunction and *EZH2* overexpression leads to abnormal expression patterns in cancer cells. *BAP1* alterations have also been shown to be associated with resistance to cisplatin-based chemotherapy in MPM [33], due to inhibition of apoptosis with a mechanism involving downregulation of E2F1.

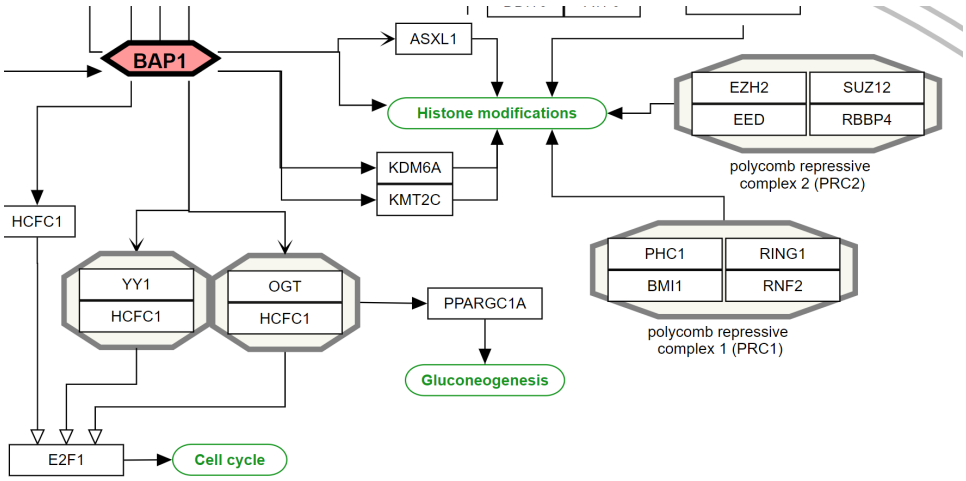

***Figure 7 - Close up pf BAP1 role in mesothelioma pathways**. Adapted from [31].*

Another very frequently mutated gene in MPM is the tumour suppressor Moesin-Ezrin-Radixin Like (*MERLIN*), also called Neurofibromin 2 (*NF2*) (28% overall in cBioPortal database, http://cbioportal.org). Its most common mutations are loss-of function mutations and deep deletions. NF2 is an inhibitor of the Hippo pathway, that ultimately leads to inhibition YAP pro-proliferating activity [34] (Figure 8). *NF2* gene's loss of function mutations therefore promote uncontrolled proliferation.

NF2 alterations potentially sensitise MPM cells to YAP inhibitors and PI3K/AKT/mTOR inhibition [35] [36]. Clinical trials with PI3K/mTOR inhibitors have shown limited activity [37] [38].

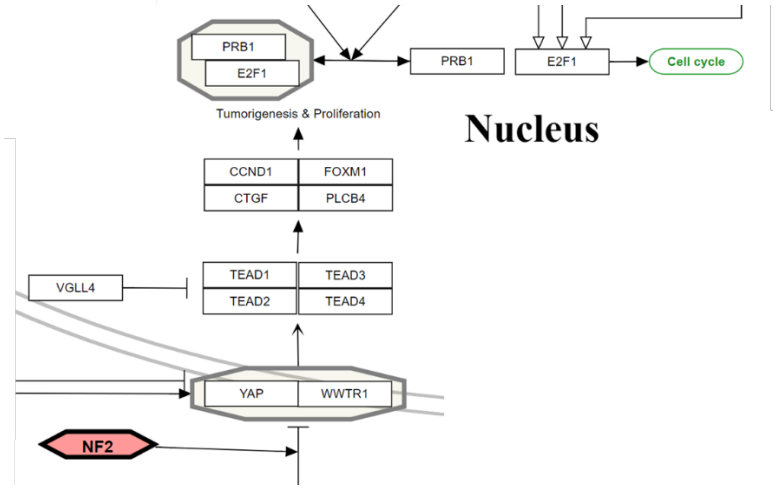

***Figure 8 - - Close up pf NF2 role in mesothelioma pathways**. Adapted from [31].*

Other genes have been reported to be less frequently mutated with loss of function such as *TP53*, *SETDB1, LATS2*, and *SETD2* [39].
Interestingly, some gain of function mutations have also been reported, like telomerase reverse transcriptase (*TERT)* copy number gains [39].

All these genetic alterations can alter tumour progression and, most importantly, the response to treatments, making MPM differently susceptible to alternative therapeutic options.

3.5 Current treatments for MPM

The different histological and molecular aspects of MPM, as well as the patient's performance status, play a role in the choice of treatment (Figure 9). Unfortunately, the aggressiveness of mesothelioma doesn't always leave space for treatment, and the only solution becomes palliative care. The

comorbidities of the patients, who are often over 70 yes old, also have to be taken into account to consider whether or not the patient is eligible for surgery.

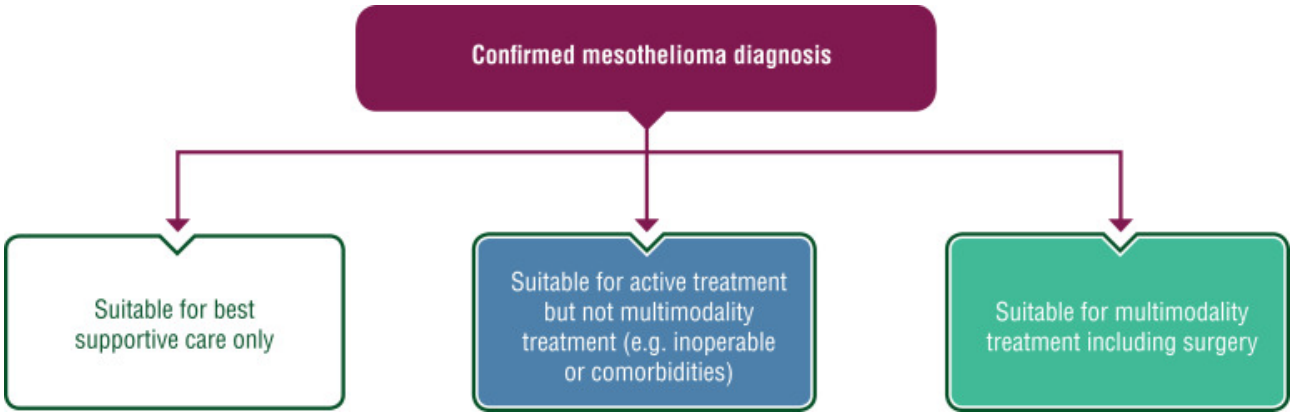

Figure 9 - Therapeutic strategy by treatment intent, a schematic approach to MPM patients' treatment. [40]

Currently, the standard of care for stage I-IIIA epithelioid MPM is surgical removal, often preceded by induction chemotherapy and followed by radiotherapy (trimodality treatment) [24].

Surgery – The surgical removal of pleural mesothelioma can be achieved through pleurectomy/decortication (P/D) or through extrapleural pneumonectomy (EPP).

P/D is currently the preferred method for removing the pleura and is performed by resecting both parietal and visceral pleura with the goal of physically removing mesothelioma's tumour mass. In case the tumour extends to the pericardium or diaphragm, parts of these can also be removed in what is called extended pleurectomy/decortication.

To be eligible for P/D, the tumour mass must be confined in one hemithorax and the procedure must not pose a too high risk to the patient, considering their health conditions prior to the operation.

The histology of the tumour is also important in determining the eligibility for P/D. Patients with biphasic or sarcomatoid mesothelioma are often considered not eligible for the procedure due to the poor overall prognosis [41].

While P/D aims at the removal of only the pleura, EPP involves the resection of the parietal and visceral pleura together with the affected lung, pericardium, and hemidiaphragm. As for P/D, pre-operative evaluation of cardiac and pulmonary functions of the patients is necessary to assess the eligibility for this procedure. Compared to P/D, EPP can be used to remove MPMs that have spread a little further than the pleura, but it can have more post-operative complications [42].

Staging of the tumour is especially important in evaluating the pros and cons of performing either P/D or EPP, since it has been shown that surgical resection of MPMs of more advanced clinical stages doesn't significantly improve the prognosis of the patients [24] [43].

Chemotherapy – The most common chemotherapeutic agent used for the treatment of MPM is cisplatin (Figure 10), a DNA damaging agent that binds to the purine bases on the DNA, thus inducing intrastrand and interstrand crosslinks causing DNA damage and challenging the DNA repair mechanisms, eventually inducing apoptosis in cancer cells [44].

Unfortunately, treatment with cisplatin alone shows low response rates of 16.7% and median survival rates of 9.3 months [45]. The low efficacy of cisplatin in eradicating the malignancy and the lack of other more effective treatments highlights the need for new solutions for this disease's treatment.

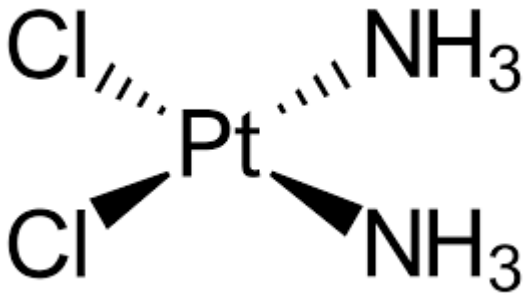

Figure 10 – cisplatin formula. *Wikipedia, https://en.wikipedia.org/wiki/Cisplatin*

Moreover, cisplatin can be the cause of frequent and numerous undesirable side effects such as severe renal insufficiency, allergic reactions, decrease in white blood cells and in immunity to infections, gastrointestinal disorders with conspicuous nausea/vomiting, hemorrhage, peripheral neuropathy, and hearing loss [44].

Currently the gold standard of chemotherapy treatment is the combination of cisplatin and pemetrexed, a folate inhibitor targeting multiple enzymes involved in folate metabolism and purine and pyrimidine synthesis. The addition of pemetrexed to the therapy has been shown to be beneficial, increasing the response rate to 41.3% and the median survival rates to 12.1 months [45]. It is important to note that pemetrexed is quite toxic in humans, where the side effects are neutropenia, anemia, thrombocytopenia, reversible bilirubin and transaminase elevation, nausea, vomiting, and diarrhea, stomatitis, renal toxicity [46]. These effects are greatly attenuated by the integration of folic acid and vitamin B12, so patient treatment must also include those two vitamins [47].

Aside from the trimodality treatment, cisplatin plus pemetrexed chemotherapy is indicated for patients that either have unresectable disease or are not eligible for surgery due to medical comorbidities or old age, which are the majority of MPM patients [48].

The addition of bevacizumab to cisplatin plus pemetrexed has significantly improved overall survival in a phase III trial, but bevacizumab has not been approved for this indication until now [49].

Radiotherapy – Radiotherapy (or radiation therapy) is a cancer treatment that uses high doses of radiation to kill cancer cells and reduce tumour size. Radiotherapy in MPM is mainly used as part of trimodality treatment. It is usually 4 to 8 weeks after completion of P/D or after the last dose of chemotherapy [50]. In case of use of EPP, radiotherapy can either be applied after EPP for stage I to III medically operable disease [50], or before EPP according to the SMART (Surgery for Mesothelioma After Radiation Therapy) approach [51]. Last, radiotherapy can be used as a palliative therapy in patients with advanced disease to reduce chest wall pain and other symptoms [50].

Immunotherapy – Tumour cells are usually seen by the immune system as foreign organisms that need to be eliminated. According to the immunosurveillance theory, the immune system continuously eradicates spontaneously arising tumour cells before they develop into detectable tumour, but sometimes this system fails, leaving the chance for the formation and development of tumours until they reach an “escape phase” where tumour cells set in place mechanisms of immune escape [51]. Immune escape can happen by selection, when tumour cells that do not express tumour antigens survive and remain untouched by the immune system (loss of antigenicity), or through

accumulation of mutations that prevent the immune response (loss of immunogenicity) or weaken it by recruiting cells that create an immunosuppressive microenvironment (Figure 11) [4].

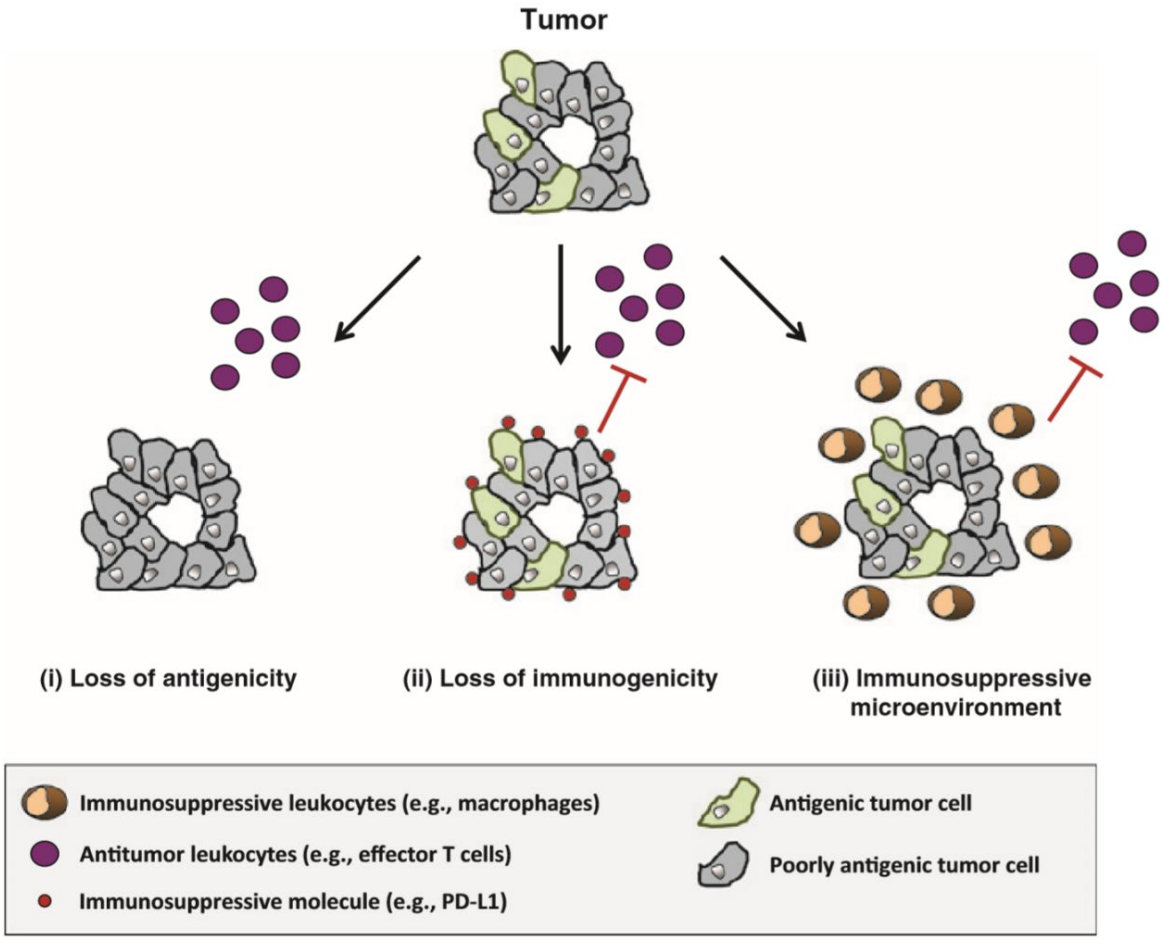

Figure 11 – Main mechanisms of escape that can develop during the growth of a tumour [4].

The efficacy of immunotherapy in the treatment of MPM is still debated. Trimodality treatment is still the advised approach for treatment of resectable tumours without the addition of any immunotherapy, but for patients with clinical stages IIIB or IV, or with any stage of sarcomatoid or biphasic histology the guidelines advise first line chemotherapy with cisplatin plus pemetrexed or immunotherapy with nivolumab plus ipilimumab [24].

Nivolumab is a fully human anti-PD1 monoclonal antibody (IgG4). It acts on the PD1/PD-L1 immune checkpoint, where programmed cell death-1 (PD1) is an immune-inhibitory receptor present on the membrane of lymphocytes that binds two ligands: PD-L1 [52], [53] and PD-L2, present on the surface of multiple tumour cell types, as well as on cells of the microenvironment [54]. The interaction between PD1 and PD-L1 acts as a negative regulator of cytotoxic T cell activity, that become unable

to recognise and effectively kill tumour cells (Figure 12) [53]. High expression of PD-L1 on tumour cells has been found to correlate with poor prognosis in MPM[55]. Nivolumab can have immune-related adverse events, which may be severe, potentially affecting any organ system, including dermatologic reactions, pneumonitis, colitis, hepatitis, endocrinopathies (especially hyper/hypothyroidism), nephritis, encephalitis, myocarditis. [56].

Ipilimumab is a monoclonal antibody that blocks the cytotoxic T lymphocyte antigen-4 (CTLA-4). CTLA-4 is a receptor that sends an inhibitory signal in T cells by binding to its ligands CD80 and CD86 present on the surface of antigen-presenting cells (APC). It is typically expressed on the surface of naïve T cells, but also on Tregs. When naïve T cells are stimulated via the T cell receptor to be activated, CTLA-4 localises to the plasma membrane, where it turns off the T cell receptor signaling [3] Immunotherapies blocking CTLA-4 prolong activation, proliferation, and amplification of T cell-mediated immune responses. Ipilimumab is burdened by the same types of immune-related toxicities seen with nivolumab, often with greater frequency and intensity, and the side effects burden is further increased when using the two drugs in combination.
Despite the activity of immune checkpoint inhibitors, the prognosis of patients with advanced disease remains poor, and new treatment options are clearly needed and being investigated (Figure 12).

Other therapies – MPM is a heterogeneous disease that varies from patient to patient. In this context, it can be useful to recognise subsets of patients with particular characteristics that make their tumour susceptible to specific therapies. One effective way to categorise the patients is based on the genetic alterations carried by their tumour, since those alteration may represent the foundations of molecular mechanisms that are vital for tumour growth and survival.
In the context of MPM, tumours carrying some of the more frequent mutations (*i*.e., in the genes *BAP1,* and *CDKN2A*) were demonstrated to be more susceptible to some treatments compared to tumours without those mutations, thus opening the way for new treatment options of at least some subsets of patients.

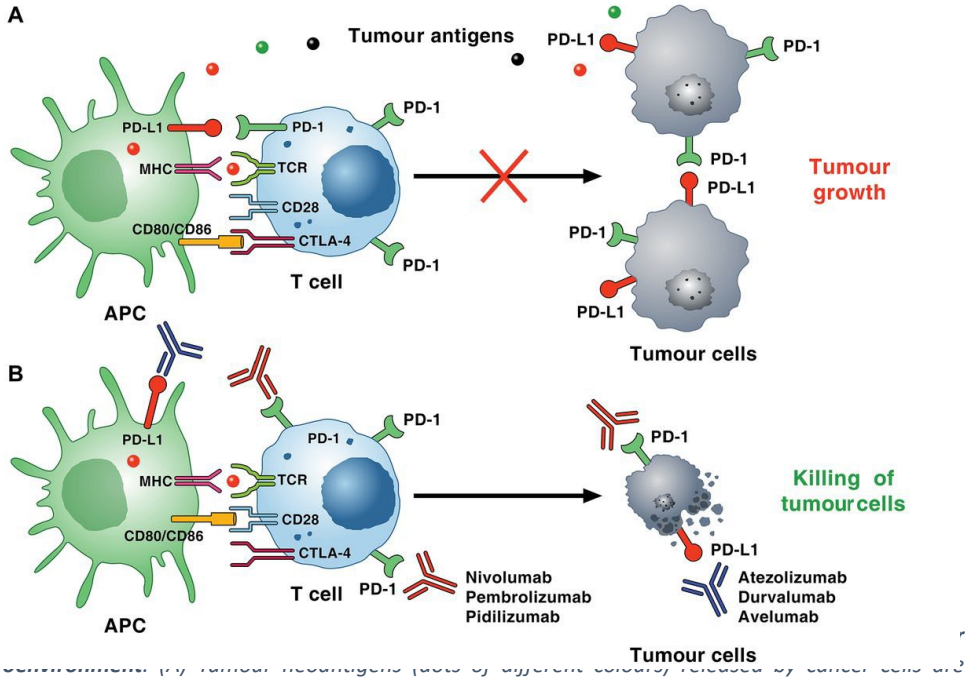

captured by APCs. These cells present peptides in the context of MHC molecules/TCRs on the surface of CD8+ cytotoxic T cells. PD1 is induced on T cells on activation through the TCR and through several cytokines. Tumour cells and other cells in the tumour microenvironment (eg, endothelial cells, mast cells) can express high levels of PDL1 and/or PDL2 that binds to PD1 on T cells, resulting in inhibitory checkpoint signalling that decreases cytotoxicity and leads to T cell exhaustion. Recent evidence suggests that murine and human cancer cell subpopulations can express PD1 and promote tumour growth. (B) PD1 blocking antibodies (nivolumab, pembrolizumab, pidilizumab and so on) inhibit the interaction of PD1 with both PDL1 and PDL2, resulting in enhanced T cell cytotoxicity, TAM activity, increased cytokine production, and ultimately killing of tumour cells. PDL1+ tumour cells can also induce T cell apoptosis, anergy, functional exhaustion and interleukin-10 production. Anti-PDL1 antibodies (atezolizumab, durvalumab, avelumab) have similar effects, but only inhibit the interaction between PDL1 and PD1. PD1, programmed cell death 1; PDL1, programmed cell death ligand 1; TAM, tumour-associaed macrophage; TCR, T cell receptor. [3]

For example, loss of function BAP1 mutations have been shown to sensitise tumour cells to EZH2 inhibition in vitro and in animal models [32]. EZH2 is an epigenetic regulator involved in the activity of Polycomb repressive complexes, that regulate chromatin compaction. This discovery led to the conduction of a phase II clinical trial with Tazemetostat, a histone methyltransferase inhibitor, in patients with relapsed or refractory MPM. This study showed a disease control rate (objective responses plus disease stabilizations) of 54% (95% CI 42–67; 33 of 61 patients) [38].

BAP1 alterations have also been shown to be associated with resistance to cisplatin-based chemotherapy in MPM [33], due to inhibition of apoptosis with a mechanism involving downregulation of E2F1.

CDKN2A loss of function alterations also impact the sensitivity to specific treatments. CDKN2A's link to the cell cycle CDK4/6-Cyclin D1 checkpoint makes tumour cells with CDKN2A loss more sensitive to CDK4/6 inhibitors in MPM [57].

Two CDK4/6 inhibitors, palbociclib and abemaciclib, were shown to be able to decrease cell proliferation in MPM cell lines and primary cultures, inducing cell cycle arrest at G1 and cell senescence [57]. Palbociclib also significantly reduced tumour growth and prolonged overall survival in MPM xenograft models [57].

A single-arm, open-label, phase 2 clinical trial with abemaciclib in patients with advanced p16ink4A-negative mesothelioma pretreated with at least one course of platinum-based chemotherapy showed at 12 weeks a disease control rate (patients with complete responses, partial responses, or stable disease) of 54% (14 out of 26 patients) (95% CI 36–71) [58]. This study showed promising clinical activity of abemaciclib in patients with p16ink4A-negative mesothelioma. Abemaciclib has therefore the potential to become a relevant therapeutic option in patients with MPM pretreated with cisplatin-based chemotherapy, and its role as first line therapy could also be explored.

Although some drugs targeting MPM cells harboring specific mutations seem to be promising, it must be kept in mind that MPM is frequently very heterogeneous, presenting subpopulations of cells with multiple different genetic alterations within the same tumour. This heterogeneity might prevent total eradication of all the tumour cell subtypes, thus leading to tumour relapse.

Drug resistance and cancer stem cells – Despite the numerous attempts at treating MPM, the complete eradication of the disease is often impossible due to the tumour acquiring resistance mechanisms to the different drugs [59].

Some mechanisms of drug resistance involve the overexpression of proteins that directly hamper the activity of the administered drugs.

For example, some transporter proteins present on cell membranes, in particular the ones called ATP Binding Cassette B1 (ABCB1) and G2 (ABCG2), have been shown to be involved in the inhibition of cisplatin's activity [60]; [61]. The expression of those proteins can be induced by the administration of cisplatin itself. Therefore, cancer cells can survive by means of acquired chemoresistance.

The complete eradication of all cancer cells after surgery and drug treatment is of utmost importance, since tumours usually contain a subpopulation of tumour cells characterised by high tumour-forming potential that, if left alive, leads to rapid recurrence of the tumour. Cells with these characteristics are called cancer stem cells.

Unfortunately, cancer stem cells sometimes are particularly resistant to chemotherapy, and subpopulation of drug-resistant cancer stem cells can also be found in MPM. Some known cancer stem cell markers, such as CD24, OCT4, and SOX2, were found to be highly expressed also in mesothelioma cells and can be used to identify mesothelioma stem cells subpopulations [62]; [63].

In this context, it may be beneficial to find a way to reduce drug resistance to the chemotherapy, so that a higher number of cancer cells would be killed by the treatment and the chance of relapse would decrease.

3.6 High throughput screenings for drug repurposing

Although chemotherapy and some other drugs can kill cancer cells and give patients a better prognosis, the effectiveness of all those treatments and the percentage of patients that respond to them are still limited. This means that the search for new treatment options for MPM must be kept going to be able to offer more effective treatments and in order to properly treat the highest possible number of patients.

The search for new treatments can follow different routes.

One way involves a targeted approach followed by drug design, where a target molecular mechanism is chosen and then a whole new molecule is designed and created to specifically interact with one or more components of that molecular pathway. This kind of approach is aimed at producing a new drug with high specificity and efficacy for treating a particular disease, which would be ideal, but it has some downsides. The design and production of the drug itself poses some challenges and has high costs [64], and the clinical development up to the approval from drug regulating authorities like the American Food and Drug Administration (FDA) or the European Medicines Agency (EMA) can take from 10 to 15 years [64].

Starting from its design, each new drug has to go through the processes of target validation, compound screening, and lead optimization, which happen *in silico* and *in vitro*. Past this step, the drug candidates go through preclinical tests on lab animals, followed by the three-consecutive clinical trials (phases I–III) which ultimately decide on the approval of the new drugs [64].

As an alternative to this lengthy and expensive approach, a more naïve approach can be used.

This approach focuses on designing functional high throughput screening (HTS) methods to test *in vitro* the efficacy of high numbers of drugs for performing specific activities. For example, biochemical assays can be designed for evaluating how different drugs affect the activity of a specific enzyme, functional assays can be designed to verify how drugs impact on a specific cellular activity, or cell vitality assays can be used to test the efficacy of drugs in killing tumour cells.

These kinds of vitality assays have already been tried for multiple types of cancer, and sometimes with the discovery of good candidate drugs for use in therapy [65]; [66]; [67].

The downside of this kind of screening is that usually there are no particular expectations on what kind of drug is going to work for the chosen purpose, if any already exists, but the advantage is that, in case of success, the researcher will have a candidate drug that is easily available and can be bought, instead of produced from scrap. Also, if the candidate drug has already been tested for safety and deemed safe to use on humans, the step of safety testing can be skipped, reducing the time and costs needed for approval in the treatment of the chosen disease.

Drug screenings addressing the ability of tested drugs to kill cancer cells have also been tried for MPM [68, 69], but at the moment none of the drugs selected through these kinds of screenings has been passed to clinical trials for MPM treatment yet.

Given that HTS methods have a high potential for identifying both relevant genes involved in crucial cellular processes and drugs with particular effects and mechanisms of action, this work focuses on designing and applying HTS approaches for researching key mesothelioma characteristics. In particular, the goal of this project is to use HTS approaches to study the role and activation of autophagy in MPM tumorigenesis, to find drugs that can downregulate the key autophagy and apoptosis regulator BCL-XL, thus affecting cancer cells survival, and to find drugs with a synergistic effect with the chemotherapeutic agent cisplatin, in order to find possible treatment options that may potentiate the effect of cisplatin while not burdening patients with additional side effects.

4. Aims

Studying many aspects of cancer pathogenesis and treatment can be a hard task. In this work, I focused on studying the application of HTS approaches to different aspects of MPM pathogenesis

since, up to date, this kind of experimental approach has been proven to be helpful in identifying molecular targets and effective drugs in many cancer models, including previous studies of MPM.

4.1 AIM1 – Investigating the role of macrophages in response to asbestos

For AIM1 I tested the effect on mesothelial cells' proliferation of factors secreted by macrophages activated by asbestos fibers. The goal was to verify whether these effects could be studied in an *in vitro* setting to deepen the knowledge on macrophages' role in the onset of MPM.

4.2 AIM2 – Investigating the role of autophagy in tumour initiation

For AIM2 I tested whether it was possible to apply an HTS approach to the study of mesothelioma onset. In particular, I attempted the establishment of a stable mesothelial cell line with a reporter for autophagy activation, a known key process in mesothelial cells survival and transformation.

4.3 AIM3 – Investigating the role of autophagy and BCL-X_L in drug resistance

For AIM3 I tested whether it was possible to apply an HTS approach to the study of mesothelioma cellular mechanisms of survival. In particular, I attempted the establishment of a stable mesothelial cell line with a reporter for BCL-X_L expression, known to be a key factor in mesothelial cells survival and drug resistance.

4.4 AIM4 – Using high throughput screenings to identify drugs synergic with current chemotherapy

For AIM4 I tested whether it was possible to apply an HTS approach to repurpose FDA-approved drugs for combination therapy with cisplatin in MPM. I designed an approach for discovery of synergistic drugs with the chemotherapeutic agent cisplatin and found possible candidates for combination therapy.

4.5 AIM5 – Validation of drug repurposing screening *in vitro*

For AIM5 I performed validation tests on the drug candidates emerged with the conclusion of AIM4 with the objective to narrow down the list of possible candidates from the list of the top hits derived from the previous screening. To this aim, the best performing drugs of the screening that were also theoretically compatible with use in combination therapy for MPM were tested for synergy with cisplatin, activity in primary mesothelioma cells, activity in a 3D setting, and modulation of known molecular processes in MPM.

5. Materials and methotds

5.1 Cell lines and cell culture.

All cell lines were kindly provided by Professor Roberta Bulla (University of Trieste, Department of Life Sciences, Immunology).

THP-1 cells were cultured in RPMI 1640 medium with 10% Fetal Bovine Serum (FBS), penicillin 100 U/mL, and streptomycin 100µg/mL (grown in suspension).

Met5A cells were cultured in RPMI 1640 medium with 10% Fetal Bovine Serum (FBS), 870nM bovine insulin, 400nM hydrocortisone, penicillin 100 U/mL, and streptomycin 100µg/mL (grown in adhesion).

NCI-H28 cells were cultured in RPMI 1640 medium with 10% Fetal Bovine Serum (FBS), penicillin 100 U/mL, and streptomycin 100µg/mL (grown in adhesion).

penicillin/streptomycin (grown in adhesion).

MSTO-211H cells were cultured in RPMI 1640 medium with 10% Fetal Bovine Serum (FBS), 300 µg/mL glutamine, and 1% penicillin/streptomycin (grown in adhesion).

Primary mesothelioma cells were cultured in HESFM medium with 10% FBS, 10ng/mL EGF, 20ng/mL basic FGF (bFGF), penicillin 100 U/mL, and streptomycin 100µg/mL (grown in adhesion).

5.2 Nuclear staining and nuclei count.

THP-1-derived macrophages – The medium was removed, and cells were fixed with 4% PFA for 10 minutes at room temperature, then washed twice in PBS. Permeabilization was performed with 0.1% Triton-X100 for 10 minutes at room temperature, then cells were washed twice in PBS and stained with HOECHST 33342 (Invitrogen catalogueH3570, used at 2ug/ml) for 10 minutes in the dark at room temperature, followed by two washes with PBS.

Met5A – The medium was removed, and cells were fixed with 4% PFA for 10 minutes at room temperature, then washed twice in PBS. Permeabilization was performed with 0.1% Triton-X100 for 10 minutes at room temperature, then cells were washed twice in PBS and stained with HOECHST 33342 (Invitrogen catalogue H3570, used at 2ug/ml) for 10 minutes in the dark at room temperature, followed by two washes with PBS.

NCI-H28 – To avoid the detachment of cells, they were fixed directly in medium by adding 32% PFA to a final concentration of 4% and incubating for 20 minutes at room temperature, then cells were

carefully washed twice in PBS. Permeabilization was performed with 0.1% Triton-X100 for 10 minutes at room temperature, then cells were carefully washed twice in PBS and stained with HOECHST 33342 (33342 (Invitrogen catalogue H3570, used at 2ug/ml) for 7 minutes in the dark at room temperature, followed by one wash with PBS.

MSTO-211H – To avoid the detachment of cells, they were fixed directly in medium by adding 32% PFA to a final concentration of 4% and incubating for 20 minutes at room temperature, then cells were carefully washed twice in PBS. Permeabilization was performed with 0.1% Triton-X100 for 10 minutes at room temperature, then cells were carefully washed twice in PBS and stained with HOECHST 33342 33342 (Invitrogen catalogue H3570, used at 2ug/ml) for 7 minutes in the dark at room temperature, followed by one wash with PBS.

Primary mesothelioma cells – HOECHST 33342 (Invitrogen catalogue H3570) was added directly in the culture medium at a final concentration of 0.2ug/ml), then cells were incubated at 37°C with 5% CO_2 for 45 minutes. After incubation, images of live cells were acquired with Operetta with Operetta fluorescence microscope (Perkin Elmer) using the dedicated Harmony software. Images were then analyzed with the Image analysis function of Columbus software.

For each cell line, HOECHST 33342 signal was detected at 450nm (blue) and images were acquired with Operetta fluorescence microscope (Perkin Elmer) at a 10x magnification using the dedicated Harmony software. Images were then analyzed with the Image analysis function of Columbus software.

5.3 THP-1-derived macrophages differentiation and polarization.

Cells of the monocytic cell line THP-1 were seeded at a density of 3*10^5 cells/well in 24-well plates in the differentiation medium RPMI 1640 with 10% FBS, 15ng/ml Phorbol Myristate Acetate (PMA), and 1% penicillin/streptomycin. Then, they were incubated at 37°C with 5% CO2 for 24h.
After 24h cells will have adhered to the plate and can be washed with PBS and incubated again for 72h in RPMI 1640 with 10% FBS and 1% penicillin/streptomycin to allow proper differentiation to THP-1-derived macrophages.

To polarise THP-1-derived macrophages towards a specific phenotype, medium was then changed as follows:

- Resting macrophages – RPMI 1640 with 10% FBS, penicillin 100 U/mL, and streptomycin 100µg/mL;
- M1 macrophages (pro-inflammatory) – RPMI 1640 with 10% FBS, 100ng/ml LPS, 500U/ml INF-γ, penicillin 100 U/mL, and streptomycin 100µg/mL;
- M2 macrophages (anti-inflammatory) – RPMI 1640 with 10% FBS, 20ng/ml IL-4, 50ng/ml IL-10, penicillin 100 U/mL, and streptomycin 100µg/mL

Cells were then incubated at 37°C with 5% CO2 for 24h.

5.4 Crocidolite fibers handling and cell treatment.

Crocidolite fibers resuspended in PBS were kindly provided by Professor Roberta Bulla (University of Trieste, Department of Life Sciences, Immunology).

Right before every experiment, the fibers' suspension was vortexed for 2minutes to ensure even distribution of the fibers in the suspension.

All the liquids containing crocidolite fibers and laboratory material that came in contact with asbestos fibers (plates, tips, etc.) were discarded in sealed containers and properly disposed of in bins for dangerous wastes, as per ISPRA guidelines [https://www.isprambiente.gov.it/files/pubblicazioni/manuali-lineeguida/MLG_125_15.pdf]

THP-1-derived macrophages – To differentiated and polarised THP-1-derived macrophages was added fresh culture medium containing crocidolite fibers to a density of 1 or 4µg/cm^2 in a final volume of 1mL/well. Cells were then incubated for 72 hours before nuclear staining or sample collection with 500µL of TRIzol reagent (Thermofisher Scientific) for subsequent RNA extraction and RT-PCR. Collected sample in TRIzol reagent were stored at -20°C for a few days before RNA extraction. For supernatant collection, the fibers were added in a final volume of 300µL/well to concentrate secreted factors.

Met5A cells – Met5A cells were seeded at a density of 100 000 cells/well in 6-well plates in Met5A culture medium and incubated at 37°C with 5% CO_2 for 24 hours to allow complete attachment to the plate. Crocidolite fibers were then added to a density of 4 or 8 µg/cm^2 and cells were incubated at 37°C with 5% CO_2 for 72h before sample collection with homemade RIPA reagent for subsequent protein quantification and Western Blot analyses. Collected samples in RIPA were stored at -80°C until quantification and analysis.

5.5 RNA extraction, DNase treatment, and reverse transcription.

Total RNA was extracted from samples collected in TRIzol reagent (Thermofisher Scientific) as per manufacturer's instructions. Briefly, 0.2 volumes of chloroform were added to thawed samples, then samples were vortexed and incubated at room temperature for 2-3 minutes. Samples were then centrifuged at 12 000xg for 15 minutes at 4°C and transparent phase was collected into a new tube. To the transparent phase was then added 1 volume of isopropanol, then samples were vortexed, incubated at room temperature for 10 minutes, and centrifuged at 12 000xg for 10 minutes at 4°C. Isopropanol war removed and the RNA pellets were washed with 1mL of 75% ethanol, then pellets were reprecipitated by centrifugation at 12 000xg for 5 minutes at 4°C. Ethanol was then removed and pellets were washed again with 1mL of 75% ethanol, followed by centrifugation at 12 000xg for 5 minutes at 4°C. Last, pellets were resuspended in 50µL of water and RNA concentration and 260/280 and 260/230 ratios were measured with NanoDrop One/One C (Thermofisher Scientific).

Extracted RNA stored at -80°C for at most 7 days before proceeding with further manipulation.

Before performing RT-PCR experiments, eventual residual gDNA was cleaned from extracted RNA with the TURBO DNA-free kit (Invitrogen).

DNase-treated RNA was reverse transcribed to cDNA with Moloney Murine Leukemia Virus Reverse Transcriptase (M-MLV RT, Invitrogen, catalogue 28025-013) used as per manufacturer's instructions.

cDNA was stored at -20°C for at most 7 days before performing RT-PCR, paying attention not to thaw it and freeze it more than once before use.

5.6 Real-Time Polymerase Chain Reaction (RT-PCR).

cDNA was diluted in demineralised water and RT-PCR was performed with QX Fast Q-PCR Master mix (SMOBio, catalogue TQ1201) as per manufacturer's instructions, using primers designed in house and purchased from Eurofins (Table 1).

Experiment	Target transcript	Primer name	Sequence 5' --> 3'
Macrophage characterization	human GAPDH	GAPDH forward	GATCATCAGCAATGCCTCCT
		GAPDH reverse	TGTGGTCATGAGTCCTTCCA
	human CD80	CD80 forward	AGGAACACCCTCCAATCTCTG
		CD80 reverse	GGTCAAAAGTGAAAGCCAACA
	human CD206	CD206 forward	CTACAAGGGATCGGGTTTATGGA
		CD206 reverse	TTGGCATTGCCTAGTAGCGTA
Response to screening selected drugs	human 18S	18S forward	ATCCCTGAAAAGTTCCAGCA
		18S reverse	CCCTCTTGGTGAGGTCAATG
	human CD24	hCD24 forward	GCAGAGCAATGGTGGCCA
		hCD24 reverse	TGGTGGCATTAGTTGGATTTGG
	human OCT4	hOCT4 forward	ATCGAGAACCGAGTGAGAGG
		hOCT4 reverse	TCGTTGTGCATAGTCGCTGC
	human p21	hP21 forward	AAGACCATGTGGACCTGTCAC
		hP21 reverse	TTCCTCTTGGAGAAGATCAGCC
	human ABCG2	hABCG2 forward	GCGACAGCTTCCAATGACC
		hABCG2 reverse	AGGATGGCGTTGAGACCAG
	human ABCB1	hABGB1 forward	GGACCGCAATGGAGGAGC
		hABCB1 reverse	CTTGTCAAGCCAATTTGAATAGCGA
	human BCL-XL	BCL-XL forward	CTTGGATGGCCACTTACCTG
		BCL-XL reverse	CAGCGGTTGAAGCGTTCC

Table 1 – Table of all used primers.

5.7 Conditioning of mesothelial cells with macrophage supernatants.

Met5A cells were seeded at a density of 50 000 cells/well in 24-well plates in Met5A culture medium and incubated at 37°C with 5% CO_2 for 24 hours to allow complete attachment to the plate, then the medium was changed with fresh Met5A culture medium and supernatant collected from THP-1-derived macrophages in a 1:1 ratio and cells were incubated at 37°C with 5% CO_2 for 72 hours. Cells were then fixed, permeabilised, and stained as indicated in the "Nuclear staining and nuclei count" section.

5.8 Western blot (WB).

For sample collection, medium on Met5A cells was removed and cells were washed once with ice cold PBS. Then, on ice, 200µL of RIPA buffer were used to collect the sample with a scraper. Samples were stored at -80°C before protein quantification and analysis.

Total protein quantification was performed with the DC protein quantification kit (Bio-rad) as per manufacturer's instructions.

For the LC3 Western Blot, 25µg of total protein were loaded on a homemade gel and run at a constant 60mA.

Running gel:

- Acrylamide-bisacrylamide mix 13.3% (mass/volume)
- Tris (pH 8.8) 375mM
- Sodium dodecyl sulfate (SDS) 0.1% (mass/volume)
- Ammonium persulfate 0.1% (mass/volume)
- TEMED 0.04% (volume/volume)

Stacking gel:

- Acrylamide-bisacrylamide mix 5% (mass/volume)
- Tris (pH 6.8) 125mM
- Sodium dodecyl sulfate (SDS) 0.1% (mass/volume)
- Ammonium persulfate 0.1% (mass/volume)
- TEMED 0.1% (volume/volume)

Proteins were transferred from gels to 0.22µm nitrocellulose membranes with Trans-blot turbo (Biorad) with the protocol for one mini gel for low molecular weight protein (1.3A, 25V, 5 minutes).

Membranes were stained with Ponceau reagent to check for correct transfer of the proteins onto the membranes, then were washed with demineralised water and TBST to eliminate the Ponceau.

Membranes were blocked by incubation with 5% BSA in TBST at room temperature for 1h with agitation.
Membranes were then cut as needed and incubated with primary antibodies:

- Anti-LC3 (rabbit IgG, Sigma, catalogue L8918), 1:1000 dilution in 5% BSA in TBST, o/n at 4°C, with agitation

- Anti-p62 (rabbit IgG, Abcam, catalogue ab91526), 1:1000 dilution in 5% BSA in TBST, o/n at 4°C with agitation

Anti-β-actin-HRP (mouse IgG, Sigma-Aldrich, catalogue A3854), 1:20 000 dilution in 5% BSA in TBST, 1h at room temperature with agitation.

After incubation with primary antibodies, membranes were washed 5 times with TBST for 5 minutes, and then incubated again with secondary antibodies:

- Anti-rabbit-HRP (goat IgG, Thermofisher Scientific, catalogue 31460), 1:500 dilution in 5% BSA in TBST, 1h at room temperature with agitation

Membranes were then washed 5 times with TBST for 5 minutes.

Protein detection was performed by using the ECL Star kit (Euroclone) as per manufacturer's instructions, then developing the signal on photography film in the dark room.

Relative quantification of the signal was done by image analysis with the software ImageJ (Fiji).

5.9 Transfection of Met5A cells with LC3-eGFP-mRFP reporter.

Met5A cells were seeded at a density of 50 000 cells/well in a 24-well plate in Met5A culture medium without antibiotics, then incubated overnight at 37°C with 5% CO_2. After incubation, cells were added a mix of plasmid DNA containing the reporter system and FuGeneHD (Promega) in a 1µg of pDNA : 3.5 µL of FuGeneHD ratio in RPMI 1640 with 10% FBS, for a total of 600ng of plasmid per well.

Cells were then incubated for 48h at 37°C with 5% CO2 before assessing transfection microscope imaging for eGFP and ,mRFP or selection of transfected cells with 500µM, 700µM, or 800µM G418.

A ptf vector plasmid containing fused LC3, eGFP, and mRFP genes under a strong CMV promoter was used for the integration of the reporter system in NCI-H28 cells. It also contained a gene for resistance to ampicillin for selection in bacteria and a gene for resistance to neomycin for selection with G418 in mammalian cells. The plasmid was kindly provided by (the Molecular Medicine unit at the International Centre for Genetic Engineering and Biotechnology, ICGEB, Padriciano, Italy).

5.10 LC3-eGFP-mRFP reporter detection.

Images were acquired with Operetta fluorescence microscope (Perkin Elmer) at 450nm (blue, HOECHST 33342), 488nm (green, eGFP), and 594nm (red, mRFP).

Transfection of NCI-H28 cells with BCL2L1-luciferase-V5 reporter.

NCI-H28 cells were seeded at a density of 3000 cells/well in a 96-well plate in RPMI 1640 with 10% FBS, then incubated overnight at 37°C with 5% CO_2. After incubation, cells were added a mix of plasmid DNA containing the reporter system and FuGeneHD (Promega) in a 1 µg of pDNA : 6 µL of FuGeneHD ratio in RPMI 1640 with 10% FBS, for a total of 100ng of plasmid per well.

Cells were then incubated for 48h at 37°C with 5% CO2 before assessing transfection with luminescence detection or selection of transfected cells with 500µM G418.

FL-BCL2L1-V5 reporter plasmid (Addgene, Plasmid #78860) (Figure 13) was used for the integration of the reporter system in NCI-H28 cells.

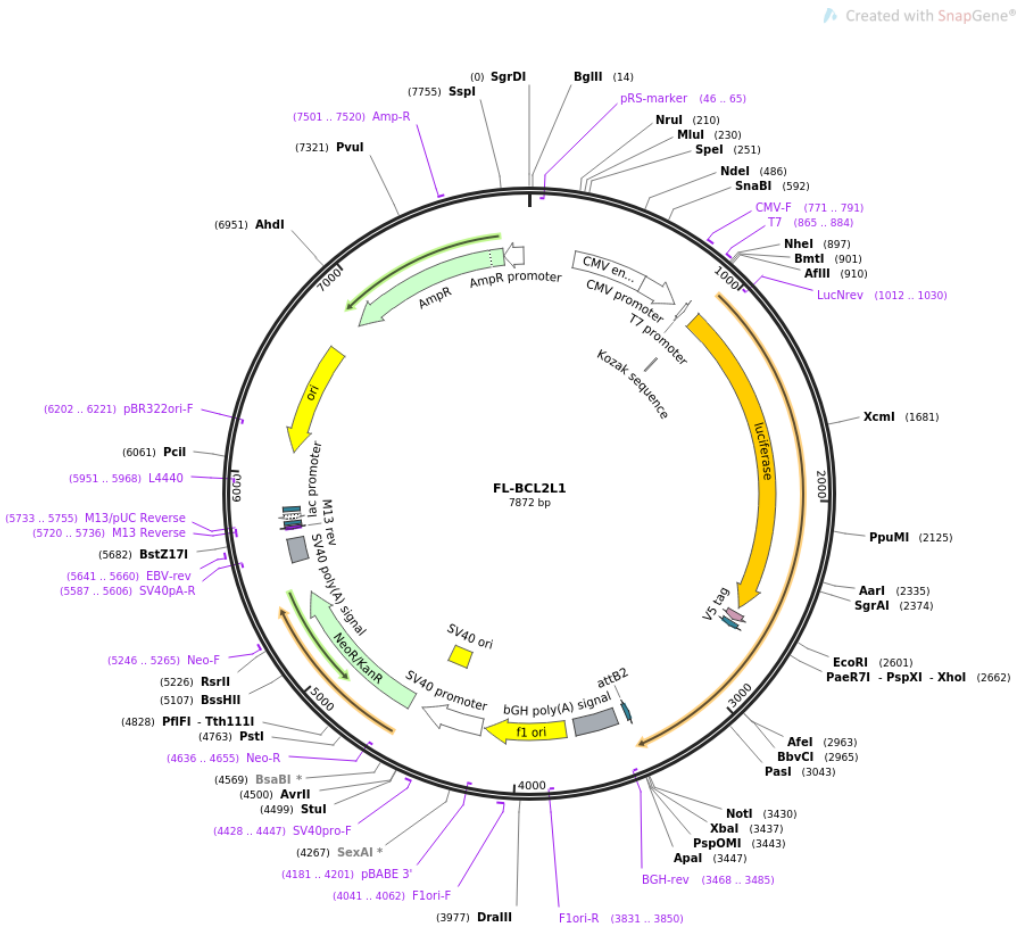

Figure 13 – Graphic representation of FL-BCL2L1-V5 plasmid. *The plasmid is a pcDNA3.1(+) vector containing fused LC3, eGFP, and mRFP genes under a strong CMV promoter. It also contained a gene for resistance to ampicillin for selection in bacteria and a gene for resistance to neomycin for selection with G418 in mammalian cells (https://www.addgene.org/78860/).*

5.11 Luciferase detection.

The signal of luciferase was detected by activating luciferase with Nano-Glo Luciferase Assay System (Promega) as per manufacturer's instructions and measuring luminescence intensity for one second with EnVision 2104 Multilabel Reader (Perkin Elmer).

5.12 Sigle clone selection with limit dilution method.

Transfected cells were detached and diluted to 20 cells/ml and seeded in 96-well plates (100ul/well, 2 cells/well) in culture medium with 500ug/ml G418 for transfected cells selection.

After overnight incubation, plates were checked and wells containing only one cell were kept under observation for cell proliferation and growth.

5.13 Resazurin-based cell viability assay.

Resazurin sodium salt (Sigma-Aldrich, catalogue R7017) was used as per manufacturer's instructions. At the end of incubation with drugs, resazurin solution in growth medium was added to the wells, then cells were incubated for 3h at 37°C with 5% CO_2 before measuring resazurin metabolization by measuring fluorescence at 560-590nm with EnVision 2104 Multilabel Reader (Perkin Elmer).

5.14 High throughput screening for drug repurposing.

The collection of drugs used for the high throughput screening was the Prestwick library of 1520 compounds, kindly provided by Prof. Stefan Shoeftner.

NCI-H28 cells were seeded at a density of 300 cells/well in preheated 384-well plates in RPMI with 10% FBS and 1% penicillin/streptomycin.

Cells were incubated overnight at 37°C to allow their complete attachment to the plates, then the 1520 drugs collection were added in the wells at the final concentrations of 2.5, 5, or 10µM with the liquid handler Microlab STARlet (Hamilton) and cisplatin was added to the wells at a final concentration of 10uM with a dispenser Multidrop combi (Thermofisher Scientific).

A scheme of the screening's settings is represented in Figure 14.

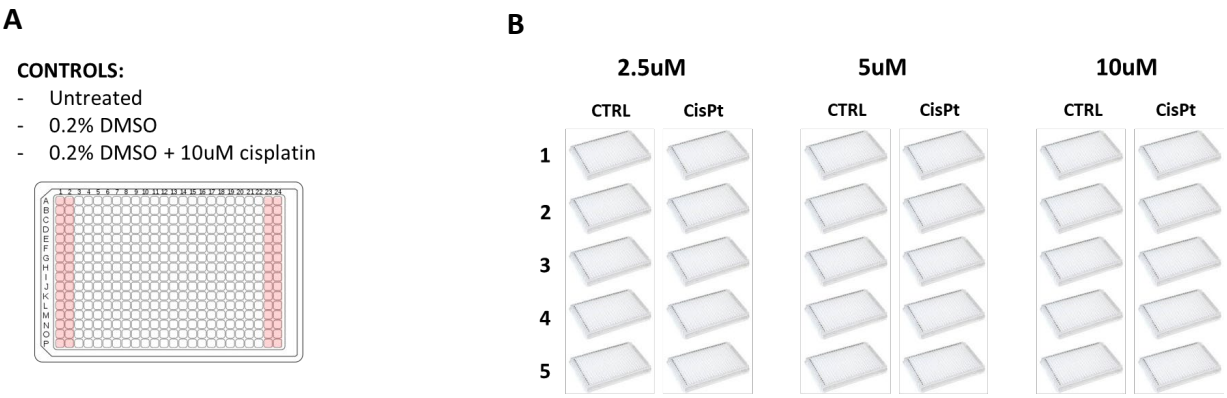

Figure 14 – Graphical representation of the HTS settings. *Wells dedicated to control conditions are colored in pink (A). Ten 384-well plates were used for each concentration of the drug library to be able to test all 1520 drugs with and without cisplatin, for a total of thirty plates (B).*

Treated cells were incubated at 37°C with 5% CO2 for 72h, then fixed, permeabilised, and stained as indicated in the "Nuclear staining and nuclei count" section.

Reagents for nuclear staining were dispensed with a dispenser Multidrop combi (Thermofisher Scientific) and removed with a dispenser/aspirator ELx405 Select CW (BioTek).

5.15 Secondary screening and hit validation

Riboflavin (CAS# 83-88-5), Proglumide (CAS# 6620-60-6), Aminosalicylic acid (CAS# 65-49-6), Gabapentin (CAS# 60142-96-3), Terfenadine (CAS# 50679-08-8), Propafenone hydrochloride (CAS# 34183-22-7), and Oseltamivir phosphate (CAS# 204255-11-8) for all validation tests were purchased as a separate batch from Prestwick.

NCI-H28 cells were seeded at a density of 800 cells/well in 96-well plates and incubated overnight at 37°C in RPMI with 10% FBS and 1% penicillin/streptomycin. Then cisplatin was added at a final concentration of 10µM, and drugs were added at different final concentrations from 0.3µM to 20µM. Cells were then incubated at 37°C with 5% CO2 for 72h and then fixed, permeabilised, and stained as indicated in the "Nuclear staining and nuclei count" section.

MSTO-211H cells were seeded at a density of 800 cells/well in 96-well plates and incubated overnight at 37°C in RPMI with 10% FBS, 300µg/ml glutamine, penicillin 100 U/mL, and streptomycin 100µg/mL. Then cisplatin was added at a final concentration of 10µM, and drugs were added at different final concentrations from 0.6µM to 20µM.

Cells were then incubated at 37°C with 5% CO2 for 72h and then fixed, permeabilised, and stained as indicated in the “Nuclear staining and nuclei count” section.

5.16 Synergy evaluation with Combenefit.

NCI-H28 cells were seeded at a density of 800 cells/well in 96-well plates and incubated overnight at 37°C in RPMI with 10% FBS, penicillin 100 U/mL, and streptomycin 100µg/mL. Then cisplatin was added at different final concentrations from 1.25 µM to 20µM and drugs were added at different final concentrations from 0.3µM to 20µM.
Cells were then incubated at 37°C with 5% CO_2 for 72h and then fixed, permeabilised, and stained as indicated in the “Nuclear staining and nuclei count” section.

MSTO-211H cells were seeded at a density of 800 cells/well in 96-well plates and incubated overnight at 37°C in RPMI with 10% FBS, glutamine, penicillin 100 U/mL, and streptomycin 100µg/mL. Then cisplatin was added at different final concentrations from 0.625µM to 10µM and drugs were added at different final concentrations from 0.3µM to 20µM.
Cells were then incubated at 37°C with 5% CO_2 for 72h and then fixed, permeabilised, and stained as indicated in the “Nuclear staining and nuclei count” section.

Synergy was calculated using the software Combenefit as per the software’s instructions with Lowe’s algorithm.

5.17 Primary mesothelioma cells isolation.

Isolated primary mesothelioma cells were kindly provided by Prof. Bulla (University of Trieste, department of Life Sciences)

Primary mesothelioma samples were received from Cattinara hospital upon retrieval of bioptic samples from patients.

Samples were washed in Hanks’ solution 1, then cut with a sterile scalpel in pieces <1mm in size. After mechanical dissociation, a solution of 5mg/mL Trypsin (Sigma-Aldrich, catalogue T4674) and 50ug/mL DNase I (Roche, catalogue 10104159001) in Hank’s solution 2 was added to the minced tissue, that was then incubated overnight at 4°C.

The day after, everything was incubated at 37°C for 30-60 minutes with agitation, then centrifuged at 1160 rpm for 7 minutes. Supernatant was discarded and pellet was resuspended in 3mg/ml Collagenase I solution in Medium 199. Tissue in collagenase solution was incubated at 37°C with agitation for 15 minutes, then the 1/5 volume of FBS was added to stop collagenase activity. The resulting medium containing digested tissue was filtered on a a 100µm cell strainer, then the filtered medium was centrifuged at 1300 rpm for 9 minutes to retrieve a pellet of cells. The pellet of cells was then resuspended in primary mesothelioma cells growth medium, and cells were seeded in tissue culture treated flasks.

After 1h cells should already start adhering to the plate and they should start proliferating a few hours later.

Isolated mesothelioma cells from each patient were either all frozen and stored at -80°C for later use, or part pf them was expanded in culture as necessary and used right away for drug validation.

All the reagents and solutions used for primary mesothelioma cells isolation are listed below:

- *DNase I* (catalogue 10104159001, Roche, Milano, Italy)
  Unmodified; final usage concentration 50µg/ml

- *Collagenase I:* collagenase type I (Worthington Biochemical Corporation, DBA, Milano, Italy)
  Unmodified; final usage concentration 3mg/ml

- *Hanks' solution 1:* Hanks' Balanced Salt Solution 1 (HBSS1, Sigma-Aldrich)
  + 1% penicillin-streptomycin (PS, Sigma-Aldrich)
  + 1:1000 fungizone (FG, Sigma-Aldrich)
  + 1:1000 gentamycin (gent, Sigma-Aldrich)
  + 1mM EDTA
  + 5mM glucose

- *Hanks' solution 2:* Hanks' Balanced Salt Solution 2 (HBSS2, Sigma-Aldrich)
  + 1% penicillin-streptomycin (PS, Sigma-Aldrich)
  + 1:1000 fungizone (FG, Sigma-Aldrich)
  + 1:1000 gentamycin (gent, Sigma-Aldrich)
  + 7,5% sodium bicarbonate (Sigma-Aldrich)

+ 1mM Ca^{2+}

+ 1mM Mg^{2+}

- *Medium 199:* Medium 199 with Hanks' salts (Sigma-Aldrich)
  Unmodified

- *HESFM medium:* Human Endothelial Serum Free Medium (Gibco, Carlsbad, CA)
  + 1% penicillin-streptomycin (PS, Sigma-Aldrich)
  + 20ng/ml bFGF (basic FGF)
  + 10ng/ml EGF
  + 10% FBS (Life Technologies)

5.18 Evaluation of markers' expression upon combination treatment.

NCI-H28 cells were seeded at a density of 270 cells/cm^2 in p100 tissue culture-treated dishes and incubated overnight at 37°C in RPMI with 10% FBS, penicillin 100 U/mL, and streptomycin 100µg/mL. Then cisplatin was added at the final concentration of 10µM, and drugs were added at the final concentration of 1.25µM. Cells were then incubated for 48h at 37°C with 5% CO_2.

MSTO-211H cells were seeded at a density of 270 cells/cm^2 in p100 tissue culture-treated dishes and incubated overnight at 37°C in RPMI with 10% FBS, 300µg/mL glutamine, penicillin 100 U/mL, and streptomycin 100µg/mL. Then cisplatin was added at the final concentration of 3µM, and drugs were added at the final concentration of 1.25µM. Cells were then incubated for 48h at 37°C with 5% CO_2.

After incubation, medium was removed and cells were washed once with PBS, then cells were retrieved with 1mL of TRIzol reagent for subsequent RNA extraction and RT-PCR. Collected sample in TRIzol reagent were stored at -20°C for a few days before RNA extraction.

5.19 Spheroids formation and treatment.

NCI-H28 cells were seeded at a concentration of 4000 cells/well in a otal volume of 200µL/well of RPMI 1640 with 10% FBS, penicillin 100 U/mL, and streptomycin 100µg/mL in Ultra-Low Attachment,

round bottom 96-well plates (Costar, catalogue 7007). Plates were briefly centrifuged at 800rpm for 2 minutes to pool all the cells in the center of the wells. No proper formation of spheroids was observed even after 4 days. Half of the medium was changed every 48h. Cells were incubated at 37°C with 5% CO_2.

MSTO-211H cells were seeded at a concentration of 4000 cells/well in a total volume of 200µL/well of RPMI 1640 with 10% FBS, 300µg/mL glutamine, penicillin 100 U/mL, and streptomycin 100µg/mL in Ultra-Low Attachment, round bottom 96-well plates (Costar, catalogue 7007). Plates were briefly centrifuged at 800rpm for 2 minutes to pool all the cells in the center of the wells. The formation of spheroids was observed already after 12h in culture. Half of the medium was changed every 48h. Cells were incubated at 37°C with 5% CO_2.

For treatment of MSTO-211H spheroids, cells were incubated for 24h after seeding, then half of the medium was removed and replaced with culture medium containing cisplatin and/or the selected drugs to reach the desired final concentrations:

Cisplatin: 3µM, 3.125µM, 6.25µM, 12.5µM, 25µM, 50µM, 100µM, 200µM.

Selected drugs (Riboflavin, Proglumide, Aminosalicylic acid, Gabapentin): 0.3125µM, 0.625µM, 1.25µM, 2.5µM.

Spheroids were incubated in presence of the drugs for 72h before size analysis.

5.20 Spheroid size analysis.

Images of the spheroids were acquired with an Olympus FE-5050 camera mounted on an Olympus CKX31 optic microscope.

Images were then elaborated and analyzed with ImageJ (Fiji) to measure the area of the section of each spheroid as follows:

1) Original images were opened in ImageJ (Figure 15).

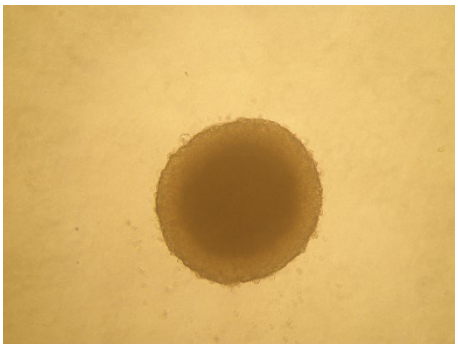

Figure 15 – Original spheroid picture.

2) Images were converted to a binary mask with Process → Binary → Convert to mask (Figure 16).

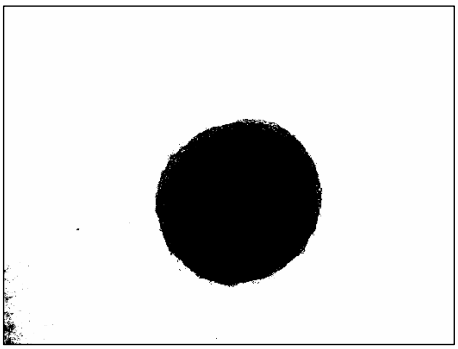

Figure 16 – Spheroid picture converted to mask.

3) Eventual holes present in the spheroids' mask were filled with Process → Binary → Fill holes (Figure 17).

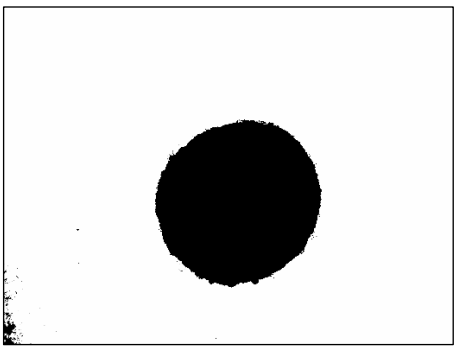

Figure 17 – Spheroid mask with filled holes.

4) Size in pixels of the spheroids' area was measured with Analyze → Analyze particles and setting a threshold from 100 000 to infinity (Figure 18).

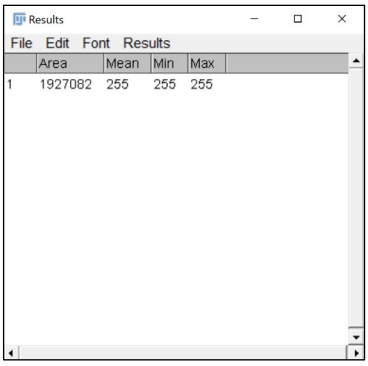

Figure 18 – Spheroid area output in pixels.

5.21 Statistical analysis.

All comparisons between multiple groups were analysed with Two-way Anova analysis with multiple comparisons using GraphPad Prism software, where significance is indicated as follows:

* $p<0.05$

** $p<0.001$

*** $p<0.0005$

**** $p<0.0001$

Cisplatin EC_{50} was calculated by normalising the number of counted cells as a percentage of the control condition and transforming cisplatin's concentrations to Log_{10}, then applying a Nonlinear fit analysis using GraphPad Prism. Confidence intervals were also calculated (data not shown).

Toxicity of the drugs alone in the screening was determined by calculating the average (DMSO Av.) and standard deviation (DMSO St.D.) of the cell numbers in all control wells (0.2% DMSO). Toxic drugs were defined as the ones producing a number of cells n° < DMSO Av. – 2*DMSO St.D.

Effectiveness of the drugs in combination with cisplatin in the screening was determined by calculating the average (Cisplatin Av.) and standard deviation (Cisplatin St.D.) of the cell numbers in all control wells (10µM cisplatin). Effective drugs were defined as the ones producing a number of cells n° < Cisplatin Av. – 2*Cisplatin St.D.

For synergy experiments, a score of the synergy for each cisplatin and drug concentration was calculated with Lowe, Bliss (data not shown), and HAS (data not shown) algorithms using the dedicated software Combenefit (https://sourceforge.net/projects/combenefit/). The three algorithms always produced comparable results (data not shown).

6. Results

6.1 AIM1 – Investigating the role of macrophages in response to asbestos.

At the beginning of my project, I focused on mesothelioma onset, trying to understand how asbestos fibers affect macrophage polarization and activation, since macrophages are cells that directly interact with asbestos fibers in their sites of deposition. To this aim, polarised and unpolarised macrophages were cultured in close contact with crocidolite fibers, then the expression of specific markers of polarization in treated and control macrophages was assessed.

To address the activation of macrophages in the presence of asbestos fibers, I decided to use crocidolite fibers, since it is an amphibole, with long, straight, and brittle fibers, and has a stronger tumorigenic effect than serpentine asbestos, which is shorter and curve and tends to stop in the upper airways and be cleared with mucus when inhaled [6].

I used THP-1-derived macrophages to test their response to contact with crocidolite fibers and I observed an activation towards the pro-inflammatory phenotype, which is characterised by an enhanced expression of the marker CD80 and a lower expression of the marker CD206 when treated with (Figure 19A,19B). The control pro-inflammatory phenotype, M1, was induced with interferon gamma and LPS treatment, while the control anti-inflammatory phenotype, M2, was induced with IL-10 and IL-4 treatment. To assess the toxicity of asbestos fibers on the cells, THP-1-derived macrophages were stained with HOECHST and the number of nuclei after the 3 days of treatment with fibers was counted. Very interestingly, treatment with crocidolite fibers of THP-1-derived macrophages also increased their numbers, suggesting that the activation of macrophages due to the contact with asbestos fibers happens on multiple levels and asbestos fibers are not particularly toxic for these cells (Figure 19C).

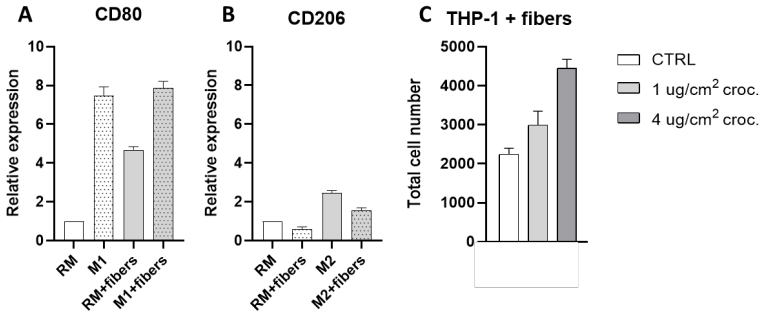

Figure 19 – THP-1-derived macrophages response to crocidolite fibers. *Relative expression of markers CD80 (A) and CD206 (B) in THP-1-derived macrophages left untreated (RM, resting macrophages), treated with M1 inducing factors, M2 inducing factors, or 1ug/cm^2 crocidolite fibers. Treatment of THP-1-derived macrophages with increasing densities of crocidolite fibers causes a dose-dependent increase in macrophage proliferation (C).*

After verifying the pro-inflammatory activation in macrophages, I assessed whether the effect of factors secreted by macrophages could affect mesothelial cells' proliferation. I used the cell line Met5A (immortalised mesothelial cells) and supernatant collected from THP-1-derived macrophages treated with either 1µg/cm^2 or 4 µg/cm^2 crocidolite fibers to assess the effect of factors secreted by macrophages on mesothelial cells' proliferation. To assess mesothelial cells' proliferation, nuclei were stained with HOECHST and were counted after the treatment with the supernatants. Mesothelial cells conditioned with macrophage supernatants collected from macrophages exposed to 1µg/cm^2 fibers proliferate the same as cells conditioned with supernatant collected from untreated macrophages, while mesothelial cells conditioned with macrophage supernatants collected from macrophages exposed to 4µg/cm^2 fibers proliferate less but the difference is not significant (Figure 20). To summarise, I did not find any specific modulation of mesothelial cells induced by asbestos-treated macrophages, even though we can observe a marked macrophage activation due to asbestos exposure. This is likely due to the long time needed for the development of this tumour, that makes it difficult to be reproduced *in vitro* in laboratory settings.

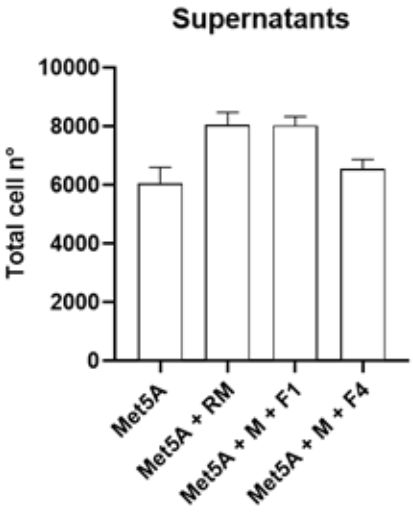

Figure 20 – Met5a proliferation in response to macrophage supernatants. *Cell count per well (96-well plates) of mesothelial Met5A cells conditioned with macrophage supernatants. Resting macrophages (RM) derived from THP-1 cells were treated with 1 ug/cm^2 crocidolite fibers (M+F1), 4 ug/cm^2 crocidolite fibers (M+F4) or left untreated as control.*

6.2 AIM2 – Investigating the role of autophagy in tumour initiation.

Autophagy is thought to play a very important role in the malignant transformation of mesothelial cells induced by asbestos fibers by promoting cell survival during DNA damage accumulation, therefore increasing the malignant transformation rate [15]. It would be of great interest to apply HTS technologies to discover, through the use of siRNA libraries, what genes are involved in the activation of this asbestos-induced process. I first confirmed that autophagy is activated by treatment with asbestos fibers. To do that, I evaluated the activation of the autophagic marker LC3

from LC3I to LC3II through western blot (Figure 3A). LC3 is a structural protein present on the surface of autophagosome vesicles which levels increase during autophagy activation [19]. LC3 is usually present in its LC3I form, that during the autophagic process is functionally modified to the lighter LC3II form, before the autophagosome fuses with lysosomes [19]. Upon treatment with crocidolite fibers, LC3 processing activation was minimal (increase of ~3 folds compared to untreated), especially when compared to the effect of chloroquine, a known inducer of autophagy, but it was consistent in biological replicates (Figure 21B). While with chloroquine there is also an increase in p62 levels, which indicates a blockade in the autophagic flux, crocidolite fibers don't seem to induce an increase in p62 levels, thus supporting autophagy flux activation (Figure 21A).

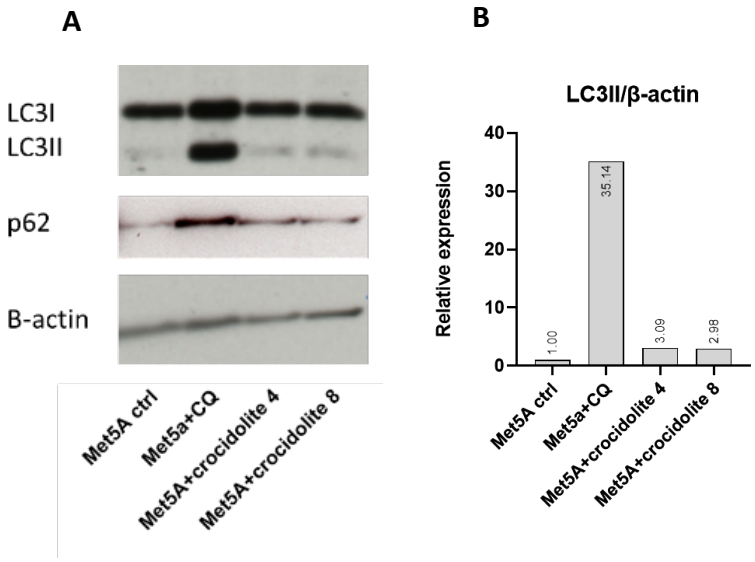

Figure 21 – Autoohagy regulation in mesothelial cells exposed to crocidolite. *Western blot analysis of autophagy activation (A) and relative quantification of activated LC3 (B)*

I then tried to set up a method for screening siRNAs that can prevent autophagy activation in mesothelial cells treated with asbestos fibers, thus revealing what genes are necessary for asbestos-induced autophagy activation. I tested a reporter model of autophagy that consists of the protein LC3 fused with red fluorescent protein (RFP) and green fluorescent protein (GFP) (Figure 22A). When the autophagic flux is active and autophagosomes fuse with lysosomes, GFP is inactivated by the acidic environment inside the fused vesicles, therefore increasing the number of red vesicles inside the cells (Figure 22B).

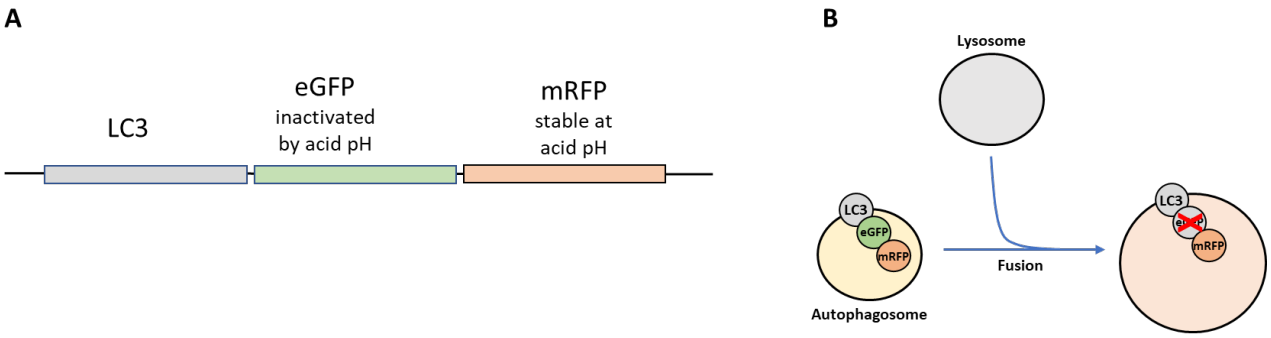

Figure 22 – The LC3 reporter. *Schematic representation of the reporter construct (A) and its mechanism of action during autophagy activation (B).*

Unfortunately, upon establishment of a stable Met5A cell line, a line derived from non-transformed mesothelial cells, expressing this reporter, the cells put in selection with G418 antibiotic survived the selection but lost the reporter after one week. Higher concentrations of G418 were tried (700µM and 800µM) for the selection of the cell line, but all the cells were unable to survive longer than 7 days. Before complete loss of the reporter in the cells that survived the selection, the selection of a single clone was attempted with the method of limit dilution, but none of the cells survived the selection.

In order to overcome this issue, I tried to setup the best conditions for the reporter's transfection and for image acquisition to verify whether it was possible to gain reliable data on autophagy activation from transiently transfected Met5A cells. Unfortunately, the images produced with cells transfected with the LC3 reporter are unsuitable to properly visualise the intracellular vesicles and quantify their numbers and fluorescence intensity. As reported in Figure 5, the differences in LC3 processing between untreated cells and cells treated with 40uM chloroquine (positive control), which is shown in Figure 3 to induce a 35-fold increase in LC3II levels compared to control, are impossible to visualise by immune staining. Therefore, given the 3-fold change induced by exposure to asbestos fibers (Figure 23) it was impossible to measure this difference through automated image analysis of immunofluorescence staining. Therefore, this method applied to NCI-H28 cells is still unsuitable for use in drug screenings performed through high throughput microscopy.

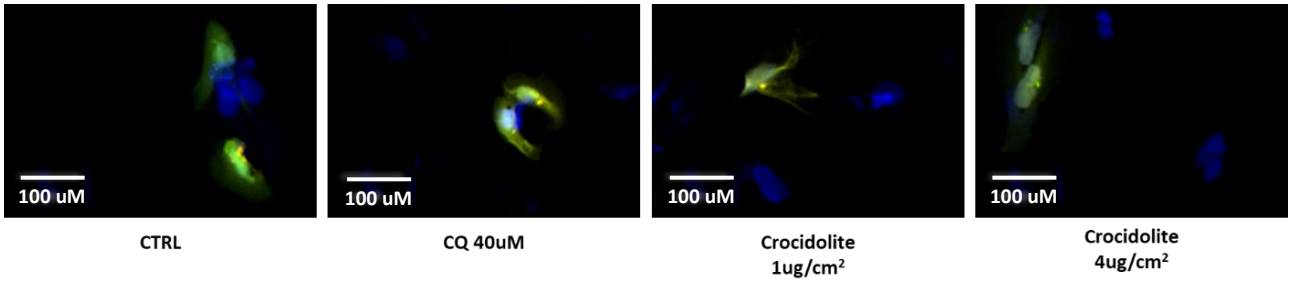

Figure 23 – Images of LC3 reporter in Met5A cells. *Visualization in fluorescence microscopy of mesothelial cells from the Met5A cell line expressing the reporter and treated with chloroquine or crocidolite fibers at different densities. The visualization and quantification of intracellular vesicles still has to be improved for applications in high throughput screenings. Nuclei are stained in blue, LC3I is represented by yellow fluorescence (red plus green), and LC3II is represented by red fluorescence.*

6.3 AIM3 – Investigating the role of autophagy and BCL-XL in drug resistance.

At this stage I tried to find alternative experimental approached to develop an HTS compatible assay to measure autophagy activation and correlate it with survival of mesothelioma cell lines. As shown by Xu *et al.,* BCL-XL is a key factor in mesothelioma cells' survival [20]. Since BCL-XL is a master regulator of autophagy and apoptosis and since its inhibition has been proven to be detrimental to mesothelioma cells' survival in vitro, finding a drug that inhibits this protein could mean finding an effective treatment for mesothelioma. Since testing newly designed inhibitors for safety and efficacy would take many years, screening a high number of drugs already approved for their use in humans to find the ones that inhibit BCL-XL could provide a faster route to finding a possible therapy.

To screen for drugs that decrease BCL-XL levels, I tried to produce stable clones of a mesothelioma cell line (NCI-H28) for a reporter BCL-XL fused with luciferase and a V5 tag.

Cells were first transfected with the plasmid containing the reporter system. The effectiveness of the transfection is confirmed by luciferase detection with a luminometer (Figure 24).

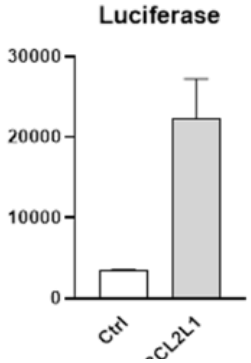

Figure 24 – Luminescence detection of CTRL and transfected samples.

I then tried to select effectively transfected cells with G418 antibiotic, but cells could not survive more than seven days, suggesting that the dysregulation of BCL-XL induced by the transfection is

already enough to hamper mesothelioma cells' survival. Since I used a reporter that is expressed under a strong promoter (cytomegalovirus, CMV), the next step towards the reporter cell line survival would be trying to insert the reporter protein under its natural promoter and after removing the endogenous non-reporter gene. This would be achievable with the CRISPR/Cas9 method, and it will be scope of future developments of this project.

6.4 AIM4 – Using high throughput screenings to identify drugs synergic with current chemotherapy.

After considering the low rate of success of the chemotherapy treatment for mesothelioma patients, I decided to focus my attention on how to make chemotherapy more effective. To this aim, I decided to exploit the same method considered for AIM3 and perform a drug repurposing screening of 1520 FDA approved drugs to identify the ones that are synergic with cisplatin, the most used chemotherapeutic agent for mesothelioma patients.

For the screening of synergy, the designed experiment included a double screening: one part consisted in treating the cells with the screened drugs only, while for the other part they were treated with the drugs plus cisplatin at its Effective concentration producing 50% of the maximal response (EC_{50}), so that cisplatin was having an effect on its own, but its effect could still be increased by the combination with a synergic drug. The part performed with the drugs only allowed us to exclude from the possible hits all those drugs that were already toxic for mesothelioma cells on their own, and thus the effect seen when combined with cisplatin was not due to synergy. Moreover, toxicity of a drug alone may also indicate that drug is toxic for cells in general, not only mesothelioma cells. This could lead to the manifestation of adverse events in patients.

In addition, since the 1520 drugs may be effective at different concentrations from one another, the entire double screening was repeated with 3 different concentrations of the library of drugs.

I chose to use the epithelioid cell line NCI-H28 because it is one of the most used for *in vitro* studies of mesothelioma. For the setting experiments, I performed seeding experiments plating different cell densities and incubating them for 24 hours. I noticed that, in the 384-well plates I would have used for the screenings, the cells were growing more slowly in the wells on the border of the plate (Figure 25A). This issue was solved by simply warming up the plates at 37°C in the incubator for a

few hours before seeding the cells (Figure 25B). To evaluate the cell numbers, the nuclei were stained with HOECHST, then images were acquired, and nuclei were automatically counted.

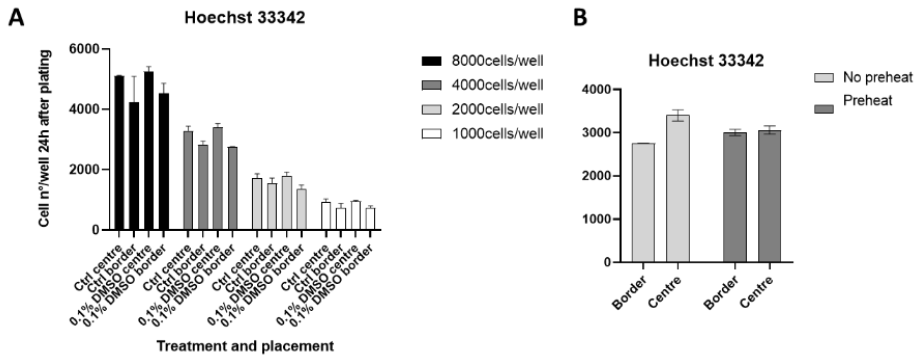

***Figure 25 – NCI.H28 seeding setting**. Seeding settings with different cell densities (A) and correction for positional differences (B).*

After solving the issue of the different growth rates in the borders of the plate, the exact number of cells to be seeded was adjusted to 300 cells/well for a 72h-long incubation as observed with nuclei staining and count (Figure 26A). A different method to evaluate cell viability was also tried. Resazurin reagent was tried as an alternative method of assessing cell viability (Figure 26B) because it is accurate, easy to use, and requires less work and time than staining, image acquisition, and automated image analysis setting and running. The two methods gave comparable results.

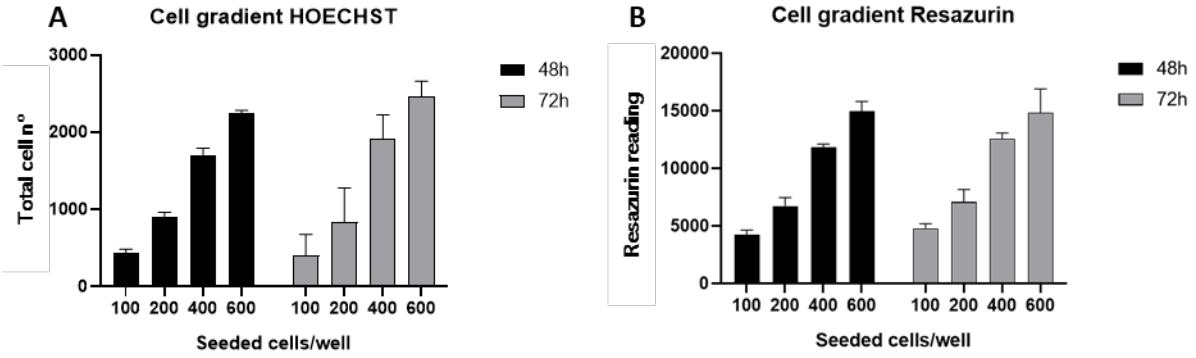

***Figure 26 – Test of cell seeding numbers for a 48h or 72h incubation.** Cell viability assessment via nuclei count (A) or Resazurin reading (B).*

After establishing the seeding conditions for NCI-H28 cells, I then tested different cisplatin concentrations on them and evaluated cell viability with both nuclei count (Figure 27A) and Resazurin reading (Figure 27B). Unexpectedly, I noticed that the Resazurin reading was not consistent with the direct count of the nuclei. There are no evidence or other instances in literature

where cisplatin hampers Resazurin's metabolism, but I decided to proceed using the count of nuclei as an output to avoid any possible trouble due to improper results given by Resazurin.

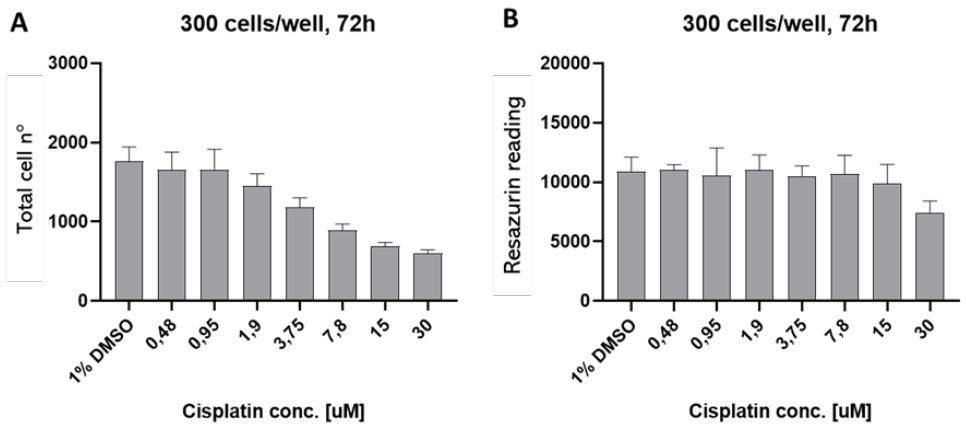

Figure 27 – There is no correspondence between nuclei count (A) and Resazurin reading (B) when cisplatin is added to the medium.

EC50 experiments performed on NCI-H28 cells seeded at 300 cells per well, incubated for 72 hours and evaluated by nuclei count revealed that cisplatin has an EC_{50} of 9.921µM (Figure 28). To simplify the work for performing all the three big screenings, this number was approximated to 10µM.

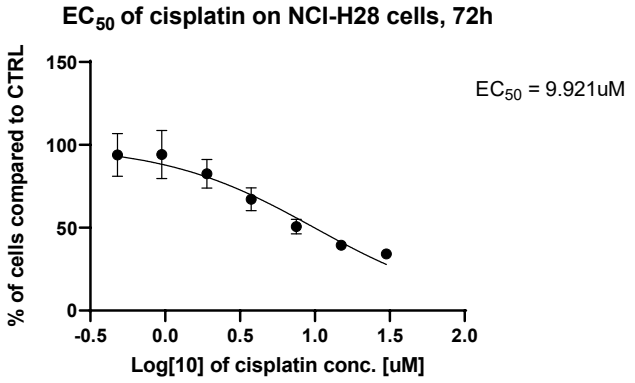

Figure 13– EC50 of cisplatin on NCI-H28 cells.

The screenings were performed by seeding the cells and incubating them overnight to let them attach to the plate. This allows the cells to initially survive all the drugs that would inhibit their attachment to the plate independently to their synergy with cisplatin. Then, the cells were treated with the drugs alone or in combination with 10µM cisplatin. The screenings were performed with drugs at the concentrations of 2.5µM, 5µM, and 10µM. After the addition of the drugs, cells were

incubated for 72 hours, then fixed and stained with HOECHST. Images were then acquired, and nuclei automatically counted.

A first selection of the synergic drugs was based on the screenings' results. Drugs were considered effective and synergic if, in combination with cisplatin, they left a number of cells equal to or less than the number of cells left by cisplatin alone – 2 standard deviations. Drugs were considered toxic non synergic if, when used alone, they left a number of cells equal to or less than the number of cells left in control condition (0.2% DMSO) – 2 standard deviations.

DMSO was used as control since all the tested drugs were dissolved in DMSO and 0.2% was the higher concentration of DMSO found in the wells of drugs given at 10µM. First, only the drugs effective and synergic at least at the concentration of 10µM were considered. Then, of those drugs, were kept only the ones that were effective and synergic but also not toxic non synergic for at least one of the three used concentrations. This selection process produced 30 drug candidates (Figure 29; Figure 30).

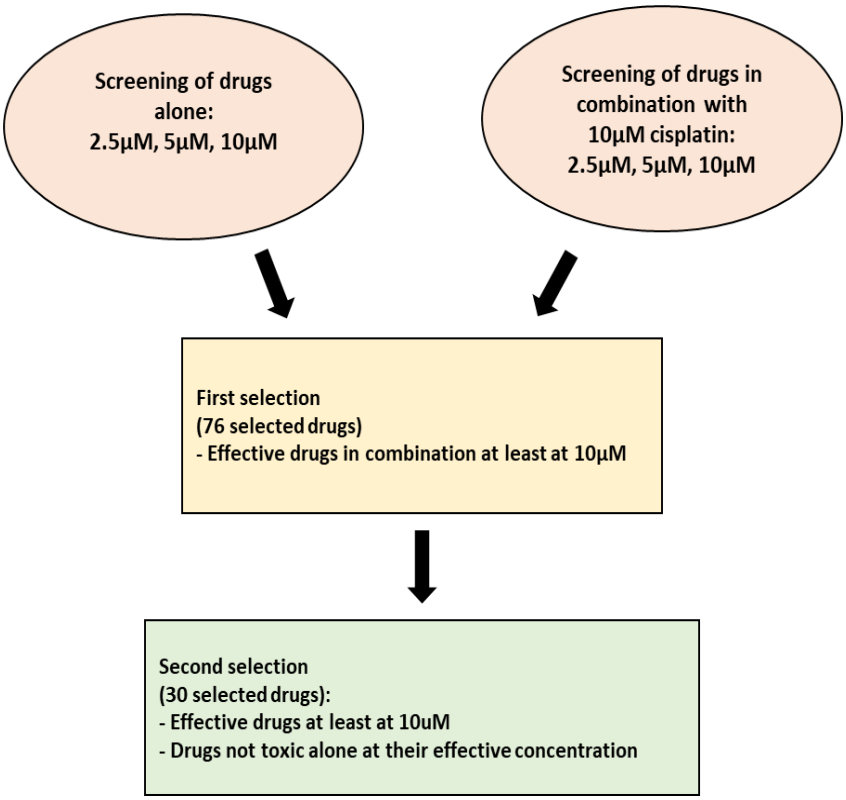

Figure 29 - Graphic representation of the screening and data analysis workflow.

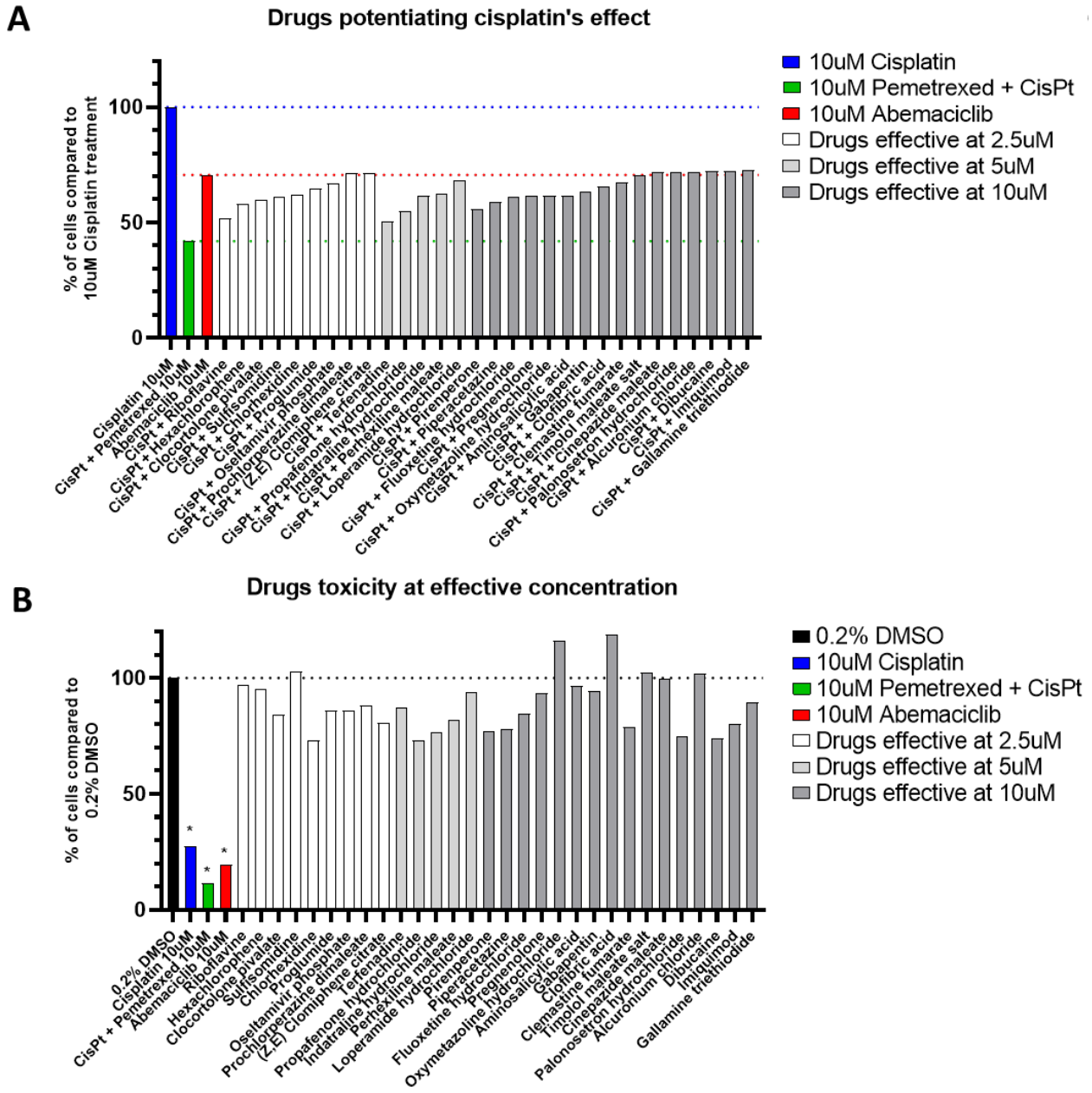

Figure 14 – Top 30 drugs selected by the screening. *Representation of the effect of effetive and synergic drugs used at their lowest effective concentration in combination with cisplatin expressed as a % of cells compared to cisplatin alone (A); Representation of the toxicity of the same drugs used alone at their lowest effective concentration expressed as a % of cells compared to 0.2% DMSO (B).*

I reported the results of pemetrexed alone and of cisplatin plus pemetrexed since the combination of these two drugs is the current standard of care. This combination was excluded by our selection because pemetrexed alone was *toxic non synergic*. This may be due to the intrinsic toxicity of pemetrexed when the vitamins B12 and folic acid are not provided [47].

As another internal control, I observed the results given by Abemaciclib, also excluded from the selection because *toxic non synergic* alone. This drug has recently been tested in a phase 2 clinical trial [58]. Although it has some side effects, Abemaciclib seems to have a good potential for treating mesotheliomas that carry a deletion of the gene *CDKN2A* [58]. In fact, it is toxic alone on the cell line NCI-H28, which is deleted for *CDKN2A*. Despite the promising results of Abemaciclib, the majority of the selected drugs was more effective in combination with cisplatin compared to Abemaciclib alone.

After the first selection, a second selection of the *effective and synergic* drugs was applied, this time based on usability in clinical practice. Drugs were excluded by this second selection based on the following criteria:

1. They had been withdrawn from the market;
2. They were only approved for use in animals;
3. They were only formulated for topical use (*i.e.,* eye drops and creams);
4. They had a mechanism of action that would result in unacceptable side effects (*e.g.,* muscle paralysis);
5. They were effective in the screening at a concentration that is not compatible with their tolerable concentration in patients' blood.

This second selection left only seven drugs as possible candidates for further testing (Figure 31):

Riboflavin (vitamin B2) – in the tissues it is converted into flavin adenine dinucleotide (FAD) and flavin mononucleotide (FMN), essential cofactors for redox reactions in cell metabolism [https://go.drugbank.com/drugs/DB00140; [70];

Proglumide (gastric ulcer treatment) – is a derivative of glutamic acid and it specifically and competitively inhibits the effects and the receptor-binding of gastrin and cholecystokinin. It has been shown that it can inhibit tumor growth in a colorectal cancer model [https://go.drugbank.com/drugs/DB13431; [71];

Oseltamivir phosphate (antiviral agent, from now on referred to as "Oseltamivir") – it exerts its antiviral activity by inhibiting the activity of the viral neuraminidase enzyme found on the surface of the virus, which prevents budding from the host cell, viral replication, and

infectivity [https://go.drugbank.com/drugs/DB00198#BE0000914]. In mammalian cells it interacts with and inhibits sialidases [72];

Terfenadine (antiallergic) – it competes with histamine for binding at H1-receptor sites in the GI tract, uterus, large blood vessels, and bronchial muscle. This reversible binding of terfenadine to H1-receptors suppresses the formation of edema, flare, and pruritus resulting from histaminic activity [https://go.drugbank.com/drugs/DB00342];

Propafenone hydrochloride (antiarrhythmic, from now on referred to as "Propafenone") – a Class 1C antiarrhythmic agent used in the management of paroxysmal atrial fibrillation/flutter and ventricular arrhythmias. It also has a weak beta-blocking activity [https://go.drugbank.com/drugs/DB01182];

Aminosalicylic acid (tuberculosis treatment) – bacteriostatic active against Mycobacterium tuberculosis tha inhibits folic acid synthesis. As bacteria are unable to use external sources of folic acid, cell growth and multiplication slows. Aminosalicylic acid may also inhibit the synthesis of the cell wall component, mycobactin, thus reducing iron uptake by M. tuberculosis. In mammalians it inhibits prostaglandin G/H synthase 2, and nuclear factor kappa-B kinase subunit alpha [https://go.drugbank.com/drugs/DB00233];

Gabapentin (antiepileptic) – an anticonvulsant medication used in the management of peripheral neuropathic pains, postherpetic neuralgia, and partial-onset seizures. It is a structural analogue of the inhibitory neurotransmitter gamma-aminobutyric acid (GABA) [https://go.drugbank.com/drugs/DB00996].

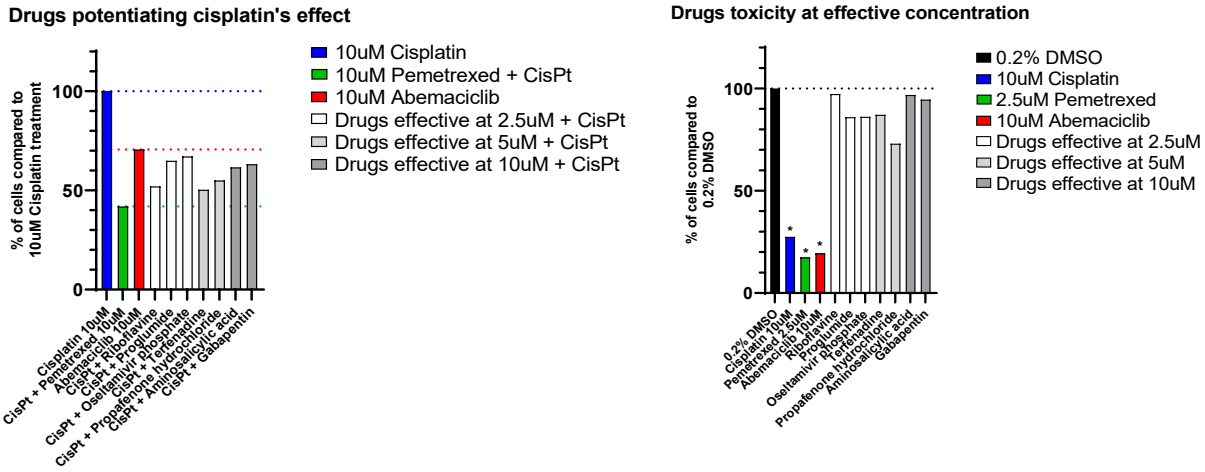

Figure 31 – Efficacy and toxicity of the top 7 chosen drugs. *Representation of the effectiveness of the seven selected drugs when used ate the lowest effective concentration in combination with cisplatin compared to cisplatin alone (A); Representation of the toxicity of the seven selected drugs when used alone compared to 0.2% DMSO (B).*

6.5 AIM5 – Validation of drug repurposing screening *in vitro.*

To validate the results of the drug repurposing screening for the seven selected drugs, I performed a secondary screening by simply testing the combination of cisplatin at 10µM with varying concentrations of the seven chosen drugs in 96-well plates, a bigger format compared to the 384-well plates used for the screening.

Once established that the proper seeding density to have a cisplatin EC_{50} of 10µM was 800 cells per well, the experiments were run on NCI-H28 cells. The tested drugs were used at final concentrations ranging from 0.3µM to 20µM.

From the first validation experiments, Terfenadine and Propafenone resulted toxic alone (Figures 32E,F), while Oseltamivir was not particularly effective (Figure 32G). On the other hand, Riboflavin, Proglumide, Aminosalicylic acid, and Gabapentin were effective already at low concentrations (Figures 32A-D).

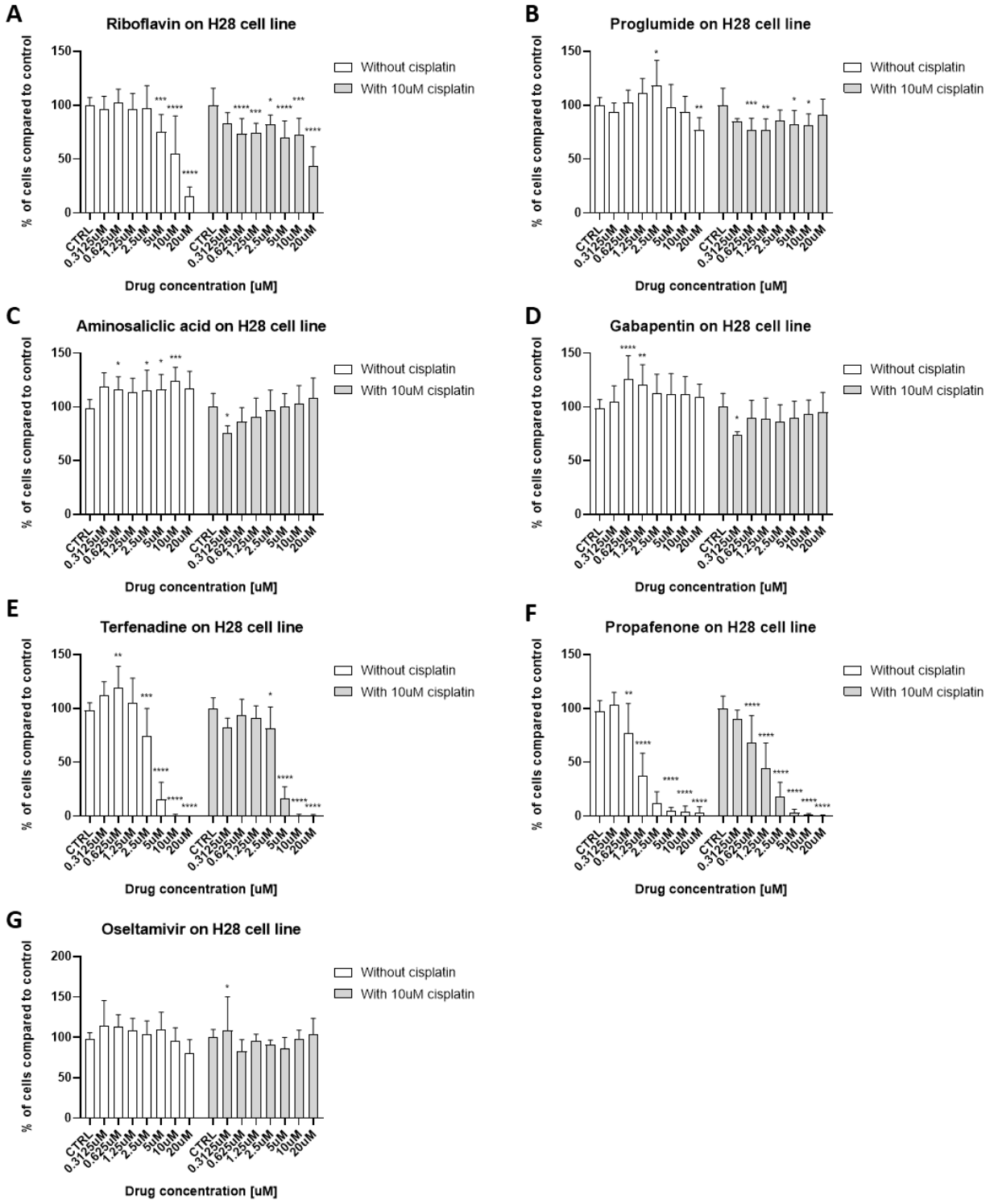

Figure 32 – Graphic representation of first validation in the NCI-H28 cell line. *Data expressed as % of live cells compared to control (0.2% DMSO in white and 10µM cisplatin in grey) for the seven chosen drugs: A) Riboflavin; B) Proglumide; C) Aminosalicylic acid; D) Gabapentin; E) Terfenadine; F) Propafenone; G) Oseltamivir.*

To assess whether the same drugs could work on mesothelioma cells with a different genetic background, the same validation experiment was performed on the biphasic mesothelioma cell line MSTO-211H. MSTO-211H cells share the same homozygous deletion of *CDKN2A* with NCI-H28 cells [73], but they are wild-type for the *BAP1* gene [74], while NCI-H28 cells carry a 23bp deletion in an intron of *BAP1* that is a loss of function mutation [75]. Once established that, at a seeding density of 800 cell per well, the cisplatin EC_{50} was 2.824µM (Figure 33) (approximated to 3µM for use in future experiments), the experiments were run on MSTO-211H cells with 3µM cisplatin.

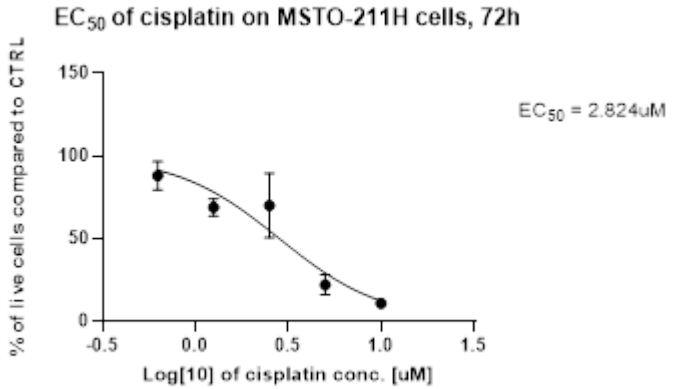

Figure 33 - EC50 of cisplatin on MSTO-211H cells.

Comparing the result to the ones of NCI-H28 cells, Riboflavin and Proglumide are less sensitive to cisplatin, showing the same synergy trend as NCI-28 cells although it is not statistically significant (Figure 34sA,B). Aminosalicylic acid's results are comparable with the ones of NCI-28 cells (Figure 34C), while Oseltamivir, that showed no significant synergy with cisplatin in NCI-H28 cells, in MTSO-211H cells shows some significance at low concentrations (Figure 34G). In MSTO-211H cells, Gabapentin seems to be the most synergic drug with cisplatin, showing significant synergy at every tested concentration (Figure 34D). Terfenadine and Propafenone are toxic alone even in MSTO-211H CELLS (Figures 34E,F).

The data obtained in the two different cell lines are not exactly comparable, suggesting that the mechanism of action of these drugs and the cell's sensitivity to the combinations with cisplatin may be affected by *CDKN2A* alterations, since the trend for each drug remains consistent but the strength of the effect can be more or less pronounced.

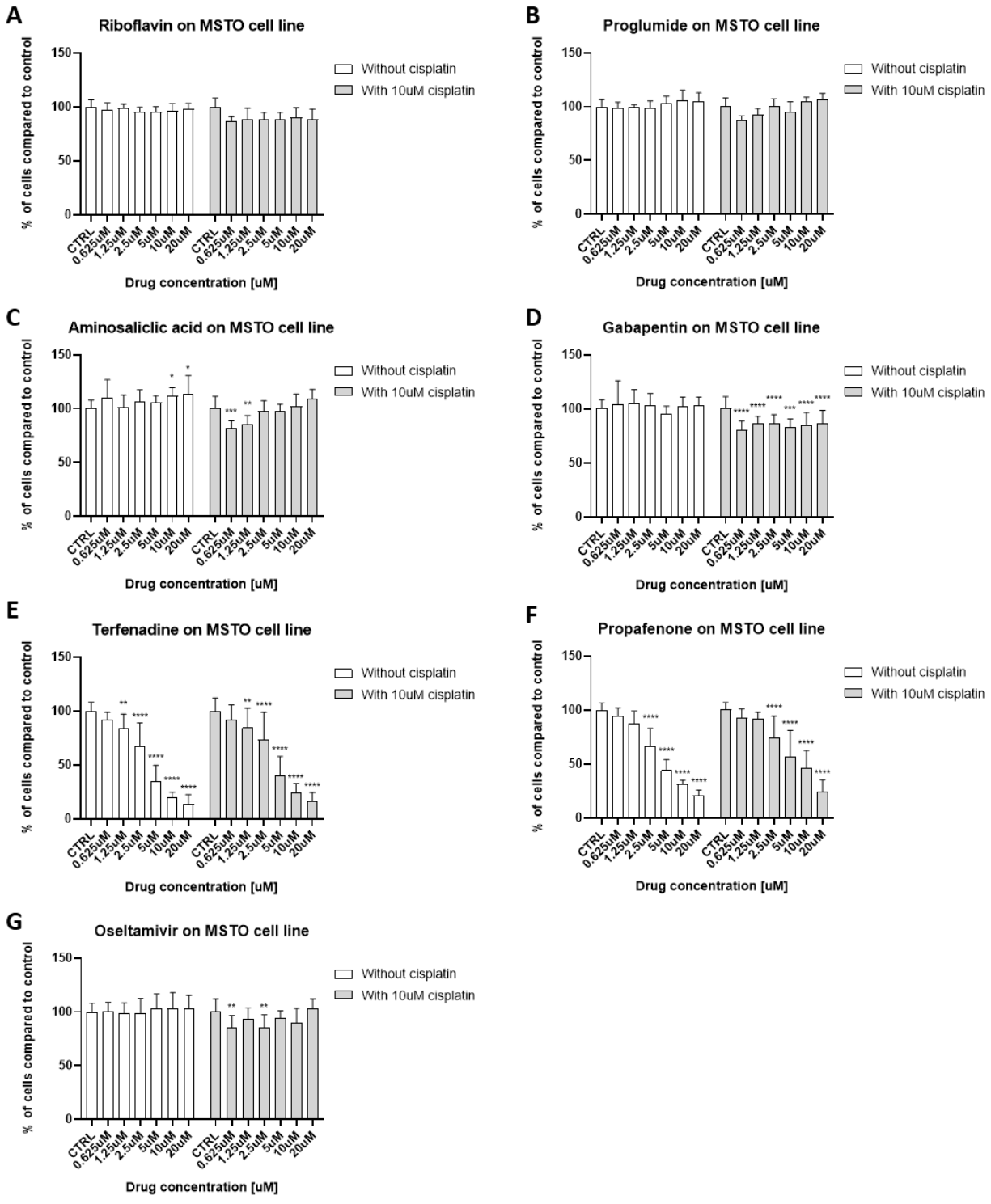

Figure 34 – Graphic representation of first validation in the MSTO-211H cell line. *Data expressed as % of live cells compared to control (0.2% DMSO in white and 10μM cisplatin in grey) for the seven chosen drugs: A) Riboflavin; B) Proglumide; C) Aminosalicylic acid; D) Gabapentin; E) Terfenadine; F) Propafenone; G) Oseltamivir.*

Since the best performing drugs were Riboflavin, Proglumide, Aminosalicylic acid, and Gabapentin, the following validation experiments were performed only for these four drugs.

An attempt at evaluating the synergy was made for the 4 top drugs by treating NCI-H28 cells with increasing concentrations of cisplatin and combined increasing concentrations of each drug, then calculating a synergy score with the software Combenefit. All the tested drugs show a significant degree of synergy at least at the highest tested concentration of cisplatin (Figure 35).

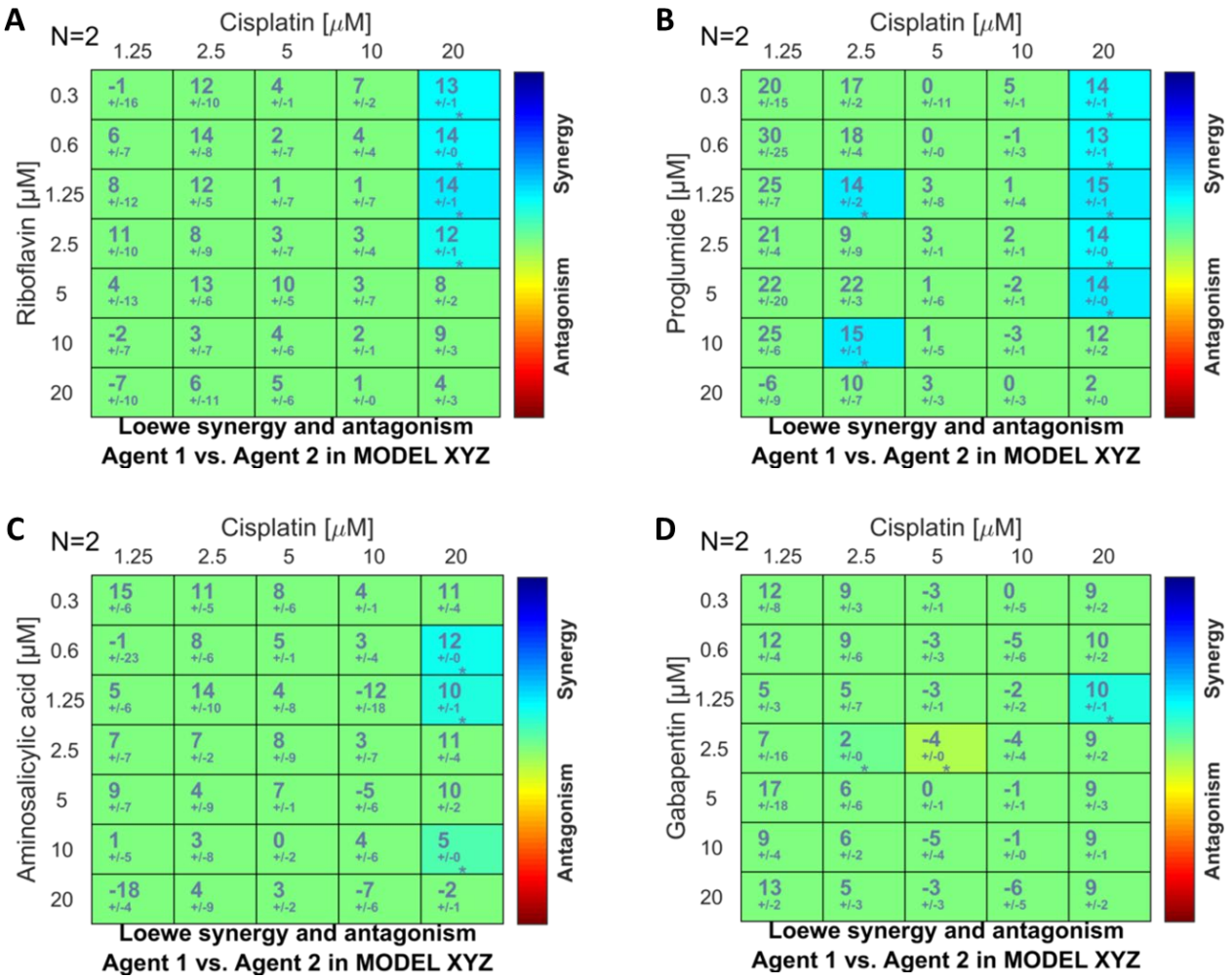

Figure 35 – Synergy analysis in NCI-H28 cells. *Lowes' synergy score for cisplatin in combination with Riboflavin (A), Proglumide (B), Aminosalicylic acid (C), and Gabapentin (D).*

The same synergy experiments were repeated for the MSTO-211H cell line, revealing that Proglumide and Gabapentin are more effective in potentiating cisplatin's effect in this cell line, while the synergic effect of Riboflavin and Aminosalicylic acid is less prominent (Figure 36). However, having only two replicates per cell line produces a bigger standard deviation, and this could make interesting scores not statistically significant. Producing more experimental replicates would increase the accuracy of this analysis.

Interestingly, Gabapentin seems to have the opposite effect as wanted when combined with the lowest cisplatin concentration (0,625µM) in MSTO-211h cells.

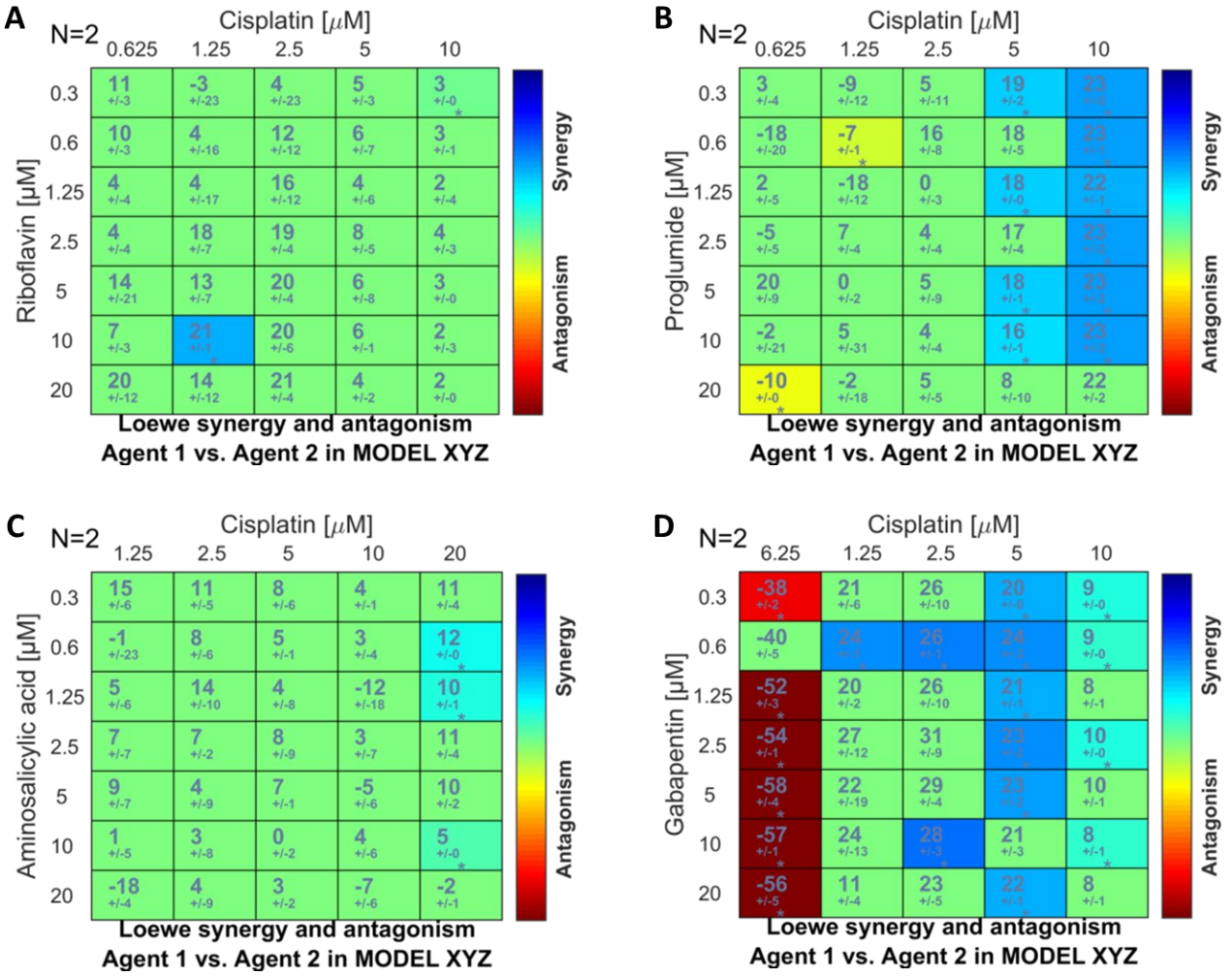

Figure 36 – Synergy analysis in MSTO-211H cells. Lowes' synergy score for cisplatin in combination with Riboflavin (A), Proglumide (B), Aminosalicylic acid (C), and Gabapentin (D) in MSTO-211h cells.

As a further step of validation, the four selected drugs were tested also on primary mesothelioma cells isolated from patients' biopsies or pleural effusions. This can give us some insight on the behaviour of the selected drugs on cells that are derived from a freshly resected piece of tumour and have not been immortalised.

Because of the large majority of MPMs being epithelial, all of the three patients had an epithelioid mesothelioma.

The cells isolated from the patients were expanded for few passages, then either frozen and stored at -80°C, then used, or directly used without freezing. For each patient, the proper seeding density and the relative cisplatin EC_{50} were assessed. Then, another experiment with drugs alone and drugs plus cisplatin at its EC_{50} was performed.

In the cells of the first analysed patient, it seems that none of the drugs had a significant synergic effect, although a trend can be observed for Riboflavin at low concentrations (Figure 37).

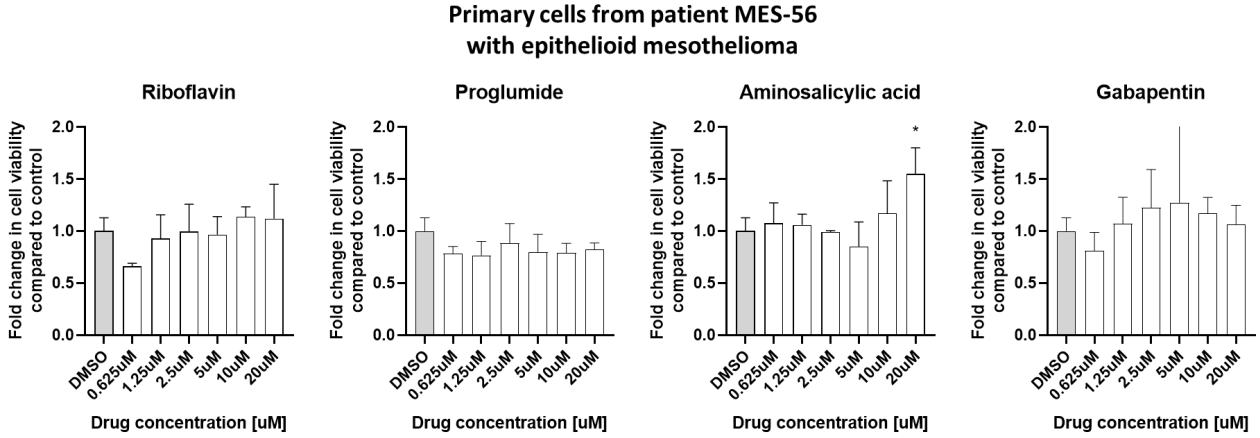

Figure 37 – Representation of cell viability expressed in fold change compared to control in patient MES-56.

In the cells of the second analyzed patient, it seems that none of the drugs had a significant synergic effect, although a slight trend can be observed for Riboflavin and Gabapentin (Figure 38).

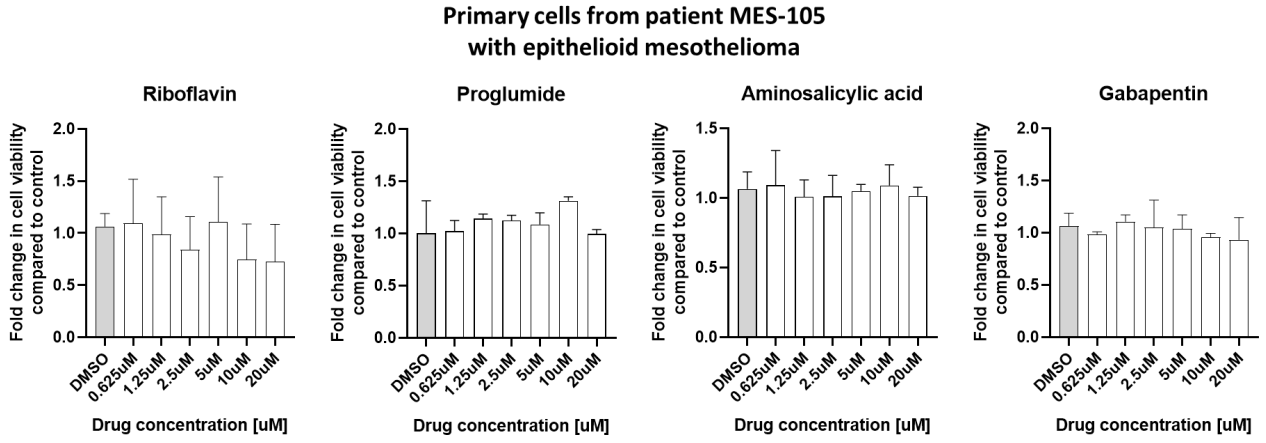

Figure 38 – Representation of cell viability expressed in fold change compared to control in patient MES-105.

In the cells of the third analyzed patient, all drugs are significantly synergic with cisplatin. Riboflavin and Proglumide are effective and synergic at every concentration. Gabapentin seems to be synergic at all concentrations but 2.5µM that is in trend but not significant. Aminosalicylic acid is effective and synergic at the lowest concentrations (Figure 39).

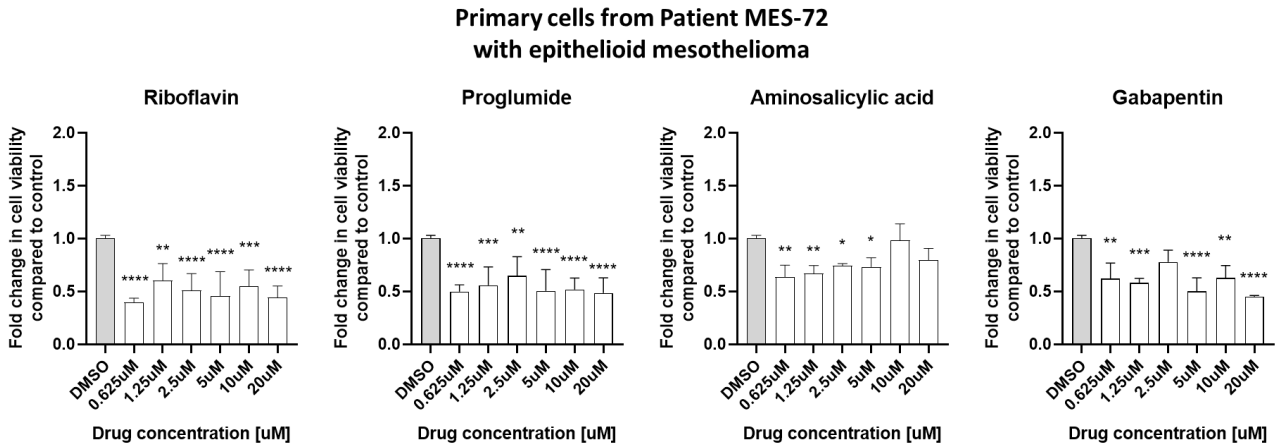

Figure 39 - Representation of cell viability expressed in fold change compared to control in patient MES-72.

The results across the primary cells isolated from 3 different patients clearly shows that selected drugs scored differently across patients , thus suggesting that clinical history and genetic background plays a crucial role in determining drug response. The state of *CDKN2A*, *BAP1*, and *NF2* in these

patients is currently unknown but will be verified to better understand their response to the tested drug combinations. A more accurate classification of the primary tumour (including genomics information) as well as a larger cohort of patients will be essential to understand efficacy of selected drugs on primary human pleural mesothelioma cells and eventually correlate gentic background with drug sensitivity.

After, I made an attempt at understanding the molecular mechanism of these drugs. A few relevant markers were selected to be analysed through RT-PCR to see if their mRNA's transcription is regulated in response to the treatment with the combination of drugs.

The chosen markers are ABCG2 and ABCB1, as they are known markers of drug resistance, CD24 and OCT4, known markers of cancer stem cells for MPM, BCL-XL, involved in autophagy and apoptosis regulation, and p21, marker of senescence.

First, NCI-H28 cells treated with 10µM cisplatin were compared to control cells to evaluate the impact of cisplatin alone in the modulation of the transcription of the selected markers. As expected from literature, treatment with cisplatin increases *ABCG2* and *p21* RNA levels, while, interestingly, it decreases the transcript of *CD24* (Figure 40A).

NCI-H28 cells treated with cisplatin alone were then compared to cells treated with cisplatin plus each drug at a concentration of 1.25µM, the most effective for each of the drugs. No significant modulation of any marker's transcript occurred, except for *ABCB1* and *OCT4*, that seemed to increase only in the presence of Aminosalicylic acid (Figure 40B). Being these markers of drug resistance and cancer stem cells, the expectation was to see them decrease, so these data need to be explored further and each drug will be tested at a range of different concentrations.

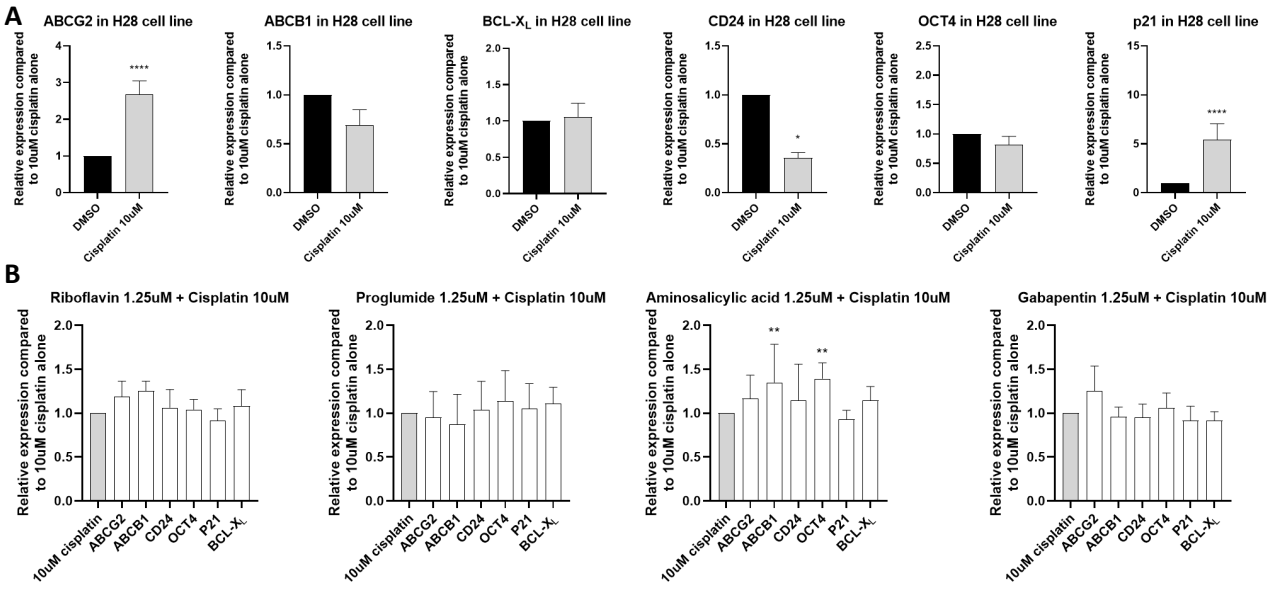

Figure 40 – Markers modulation by drugs combination on NCI-H28 cells*. Representation of selected markers' modulation in response to cisplatin compared to 0.2% DMSO (A) . Representation of selected markers' modulation in response to each drug in combination with cisplatin expressed as fold change compared to their expression in cisplatin alone (represented as a grey column set to 1) (B).*

The same experiments were performed on MSTO-211H cells treated with 3µM cisplatin and compared to control cells. As expected from literature, treatment with cisplatin increases *p21* RNA levels, while, unexpectedly, the expression of drug resistance markers remains unaltered. Also, on the contrary of what happens in NCI-H28 cells, treatment with cisplatin alone seems to increase the level of *CD24* transcript, suggesting that cancer stem cells of this cell line are less subject to cisplatin-induced death (Figure 41A).

MSTO-211H cells treated with cisplatin alone were then compared to cells treated with cisplatin plus each drug at a concentration of 1.25µM, the most effective for each of the drugs. The RNA levels of *ABCB1* and, more markedly, of *CD24* seem to decrease, albeit the decrease is statistically significant only for *CD24* in presence of proglumide and Gabapentin (Figure 41B). In this cell line, the efficacy of the top four drugs could be explained by a possible cancer stem cells-killing activity, that balances the tendency of these cells of surviving more to cisplatin alone.

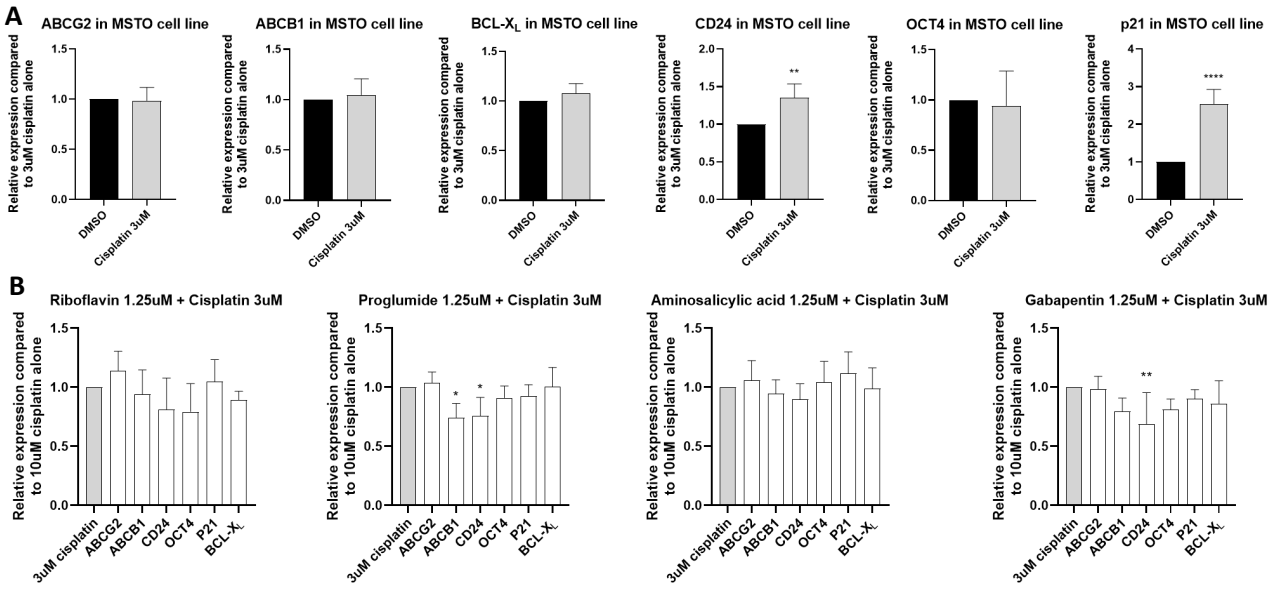

***Figure 41 - Markers modulation by drugs combination on MSTO-211H cells**. Representation of selected markers' modulation in response to cisplatin compared to 0.2% DMSO (A) . Representation of selected markers' modulation in response to each drug in combination with cisplatin expressed as fold change compared to their expression in cisplatin alone (represented as a grey column set to 1) (B).*

Although it is quite interesting to observe the mRNA levels of a marker, the Real-Time PCR alone is not informative enough. To understand the actual quantity changes in the proteins of interest, a Western Blot analysis should be performed, since it takes into account the balance between protein production and protein degradation. Western Blot analyses of the aforementioned markers will be performed to be sure about their modulation in combination treatment, but different mechanisms of action should also be considered.

To further validate the effect of the chosen drugs on mesothelioma cells, I set up a three-dimensional culture of spheroids. NCI-H28 cells and MSTO-211H cells were seeded in round bottom ultra-low attachment plates to allow the formation of spheroids. Since the NCI-H28 cells don't seem to be able to produce proper spheroids, only the MSTO-211H cell line was used for further experiments in a 3D setting (Figure 42).

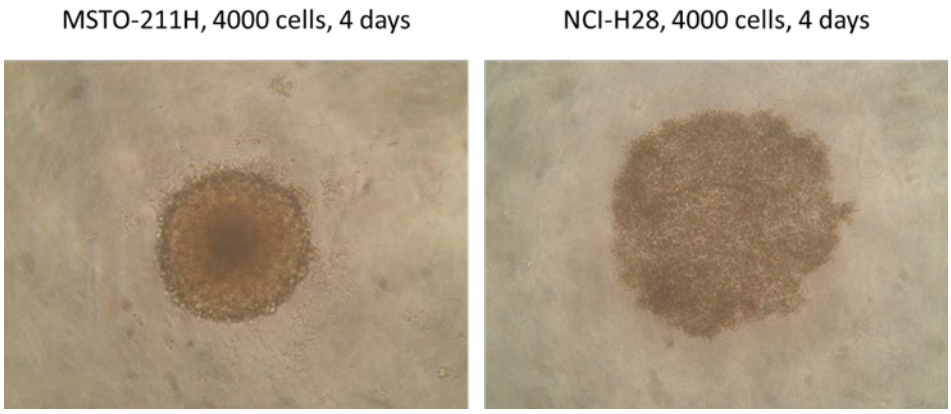

Figure 42 – Pictures of MSTO-211H (left) and NCI-H28 (right) spheroids taken at an optic microscope.

After setting the seeding density of 4000 cells per well (96/well plate) in 200µL of medium as the proper condition to obtain MSTO-211H spheroids of a good size after four days in culture, cells were seeded, then incubated for 24 hours to allow the initial formation of the spheroid. Next, the spheroids were treated with increasing concentrations of cisplatin for 72 hours (Figure 43).

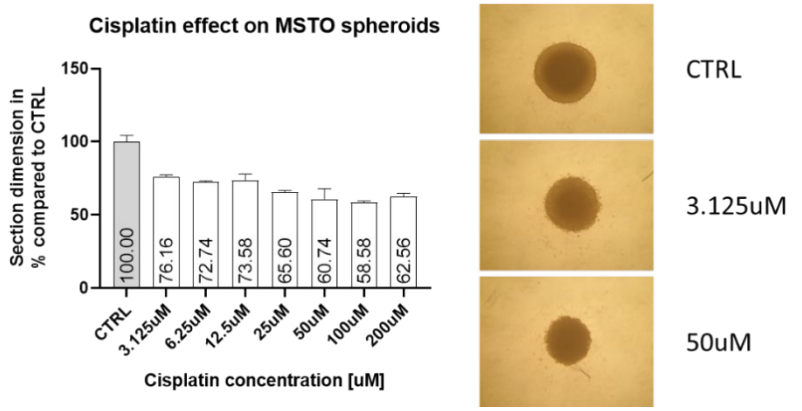

Figure 43 – MSTO-211H spheroids response to cisplatin. *Analysis of spheroid size expressed as % of control condition. The size was measured in pixels as area of the spheroid section.*

Spheroid size reaches a plateau after 50µM cisplatin where the area of the spheroid's section does not decrease below around 60% compared to control. To allow the drugs to show their effect in subsequent experiments, I decided to treat spheroids with 3µM cisplatin to have a size that is still bigger than 75% of control's size.

To test the drugs, MSTO-211H spheroids were treated with different concentrations of drugs alone or in combination with cisplatin. In the preliminary experiment, none of the drugs at any concentration had any effect, either alone or in combination with cisplatin (Figure 44A, B). Experimental conditions will be adjusted, and the experiment will be repeated to assess a larger range of concentrations. In particular, given the 20-fold decrease in the sensitivity of organoids to

cisplatin compared to 2D cultured mesothelioma cells (respectively 50µM vs 3µM to get 60% reduction in viability) we will increase accordingly the concentration of selected drugs in order to test a proportional range of concentrations.

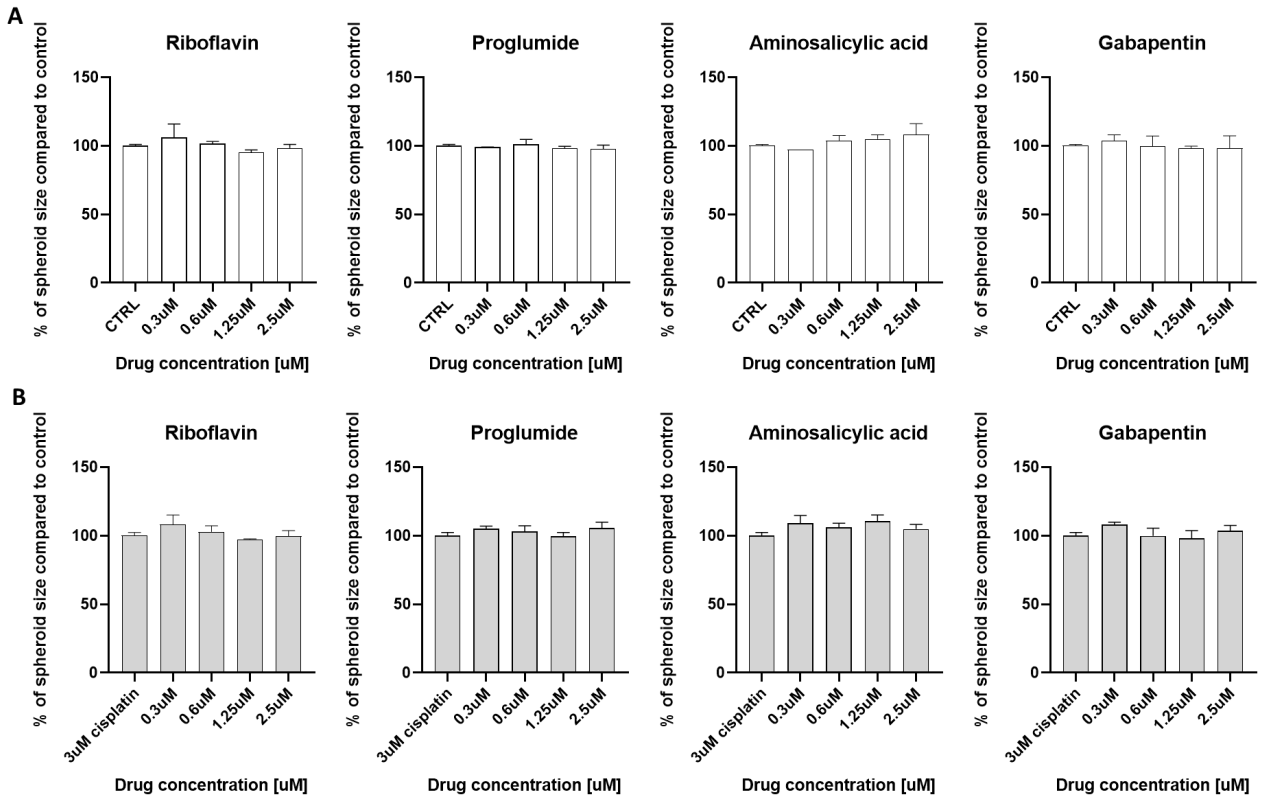

Figure 44 – Analysis of spheroid size expressed as % of control condition. *The size was measured in pixels as area of the spheroid section. (A) Comparison of drugs alone with 0.2% DMSO. (B) Comparison of drugs plus 3µM cisplatin with 3µM cisplatin alone.*

In conclusion, further analyses need to be performed to fully understand why the selected work in synergy with cisplatin. Despite this, the synergistic effect in mesothelioma cell lines is undeniable, especially for three out of the four selected drugs. In particular, Proglumide is the drug with the most consistent synergistic effect throughout the experiments and resulted especially powerful in the synergy experiments with the Combenefit analysis. In addition to Proglumide, Riboflavin and Gabapentin should be considered for further testing, since their synergistic effect with cisplatin is also pretty consistent, although less powerful than Proglumide. Furthermore, they would be perfect candidates for use in humans as combination therapies with cisplatin since Riboflavin (vitamin 2) and Gabapentin have already been proved to be safe to use together with this chemotherapeutic agent in animals and humans [76]; [77]; [78]; [79].

7. Discussion

Malignant pleural mesothelioma is a complex disease that has yet to be understood under many aspects. The onset of this disease is particularly hard to understand due to the long time that passes between exposure to asbestos fibers, the main etiologic factor of this disease, and the actual onset of the disease, that manifests decades later. Analyzing how cells interact with asbestos may shed light on the mechanisms of tumour onset. In particular, macrophages are known to directly come in contact inhaled asbestos fibers in the lungs [12]; [13]; [14], where they try to eliminate them as foreign objects. In this work, I demonstrated that macrophages exposed to asbestos fibers are induced to shift towards a pro-inflammatory phenotype. This finding supports the hypothesis that the deposition of asbestos fibers in the tissues leads to a state of local chronic inflammation that, with time, promotes cell transformation. Despite the induced pro-inflammatory state and the frustrated phagocytosis, macrophages numbers seem to increase when they are exposed to increasing concentrations of asbestos fibers, suggesting that the intrinsic toxicity of asbestos fibers may be overcome by the activation of macrophages, which proliferate more.

The toxicity of asbestos fibers is, on the contrary, not well tolerated by mesothelial cells, that tend to die more with increasing asbestos fibers concentrations [15]. It is thought that mesothelial cells exposed to asbestos fibers can activate survival mechanisms to escape asbestos-induced death [15]; [20], so they will have a higher chance of transforming due to the DNA damage done by asbestos. But what is the contribute of the pro-inflammatory signals released by macrophages to mesothelial cells survival and proliferation? Using supernatants collected from macrophages exposed to asbestos fibers, I observed that mesothelial cells treated with said supernatants didn't have significant changes in proliferation. But it must be kept in mind that mesothelioma is a disease that develops decades after asbestos exposure. Therefore, the poor modulation observed in mesothelial cells proliferation can be due to the experimental conditions, that only allow treatments of a few days for *in vitro* experiments.

To further characterise the role of autophagy activation in mesothelioma onset, I first verified that the cell line I was using for my experiment was actually able to activate the autophagic flux in the presence of asbestos cells by comparing the protein levels of LC3II and p62 in treated versus control Met5A cells. Once this asbestos-induced activation was confirmed, I designed a high throughput screening (HTS) with the goal of understanding what genes are involved in asbestos-induced autophagy activation. The idea was to use a cell line expressing a fluorescent reporter of autophagic

flux and expose it to asbestos fibers. Then, the treated cells would have been transfected with a library of siRNAs and checked for autophagy activation, thus revealing what genes are necessary for this cellular process. Unfortunately, some technical difficulties were encountered. First, the production of a stable cell line expressing the LC3 reporter system was not well tolerated, since cells transfected with the plasmid containing the reporter were unable to survive the clones' selection process. This could be due to the toxicity of the reporter system itself in this specific cell line. To avoid this issue, I tried to proceed with transiently transfected Met5A cells with the same reporter, but another issue arose. In fact, no difference in LC3 levels were observed between control and chloroquine treated Met5A cells, that was instead confirmed by western bot analyses. So, it appears that this reporter may not be sensitive enough to measure neither big nor small changes in the levels of autophagic flux activation, at least in this cells line and with the utilised image acquisition method (Operetta, Perkin Elmer), making this system not yet suitable for application in functional screening.

To develop a different approach for using HTS in the study of MPM, I then focused on the study of autophagy activation and its correlation with survival of mesothelioma cell lines. It is in fact known that autophagy plays a critical role also in the survival of transformed mesothelioma cells. In particular, it is regulated by the key factor BCL-X_L, a master regulator of both autophagy and apoptosis [20]. To this aim, I designed a functional HTS involving the use of NCI-H28 mesothelioma cell line stably expressing a reporter of BCL-X_L fused with firefly luciferase. The goal of the screening would have been identifying drugs that could induce a reduction of BCL-X_L protein levels, measurable by detection of luciferase levels in the reporter cell line. This project also encountered some difficulties, since NCI-H28 cells were successfully transfected with the reporter system, but they also were unable to survive over 7 days of clone selection and were unable to properly proliferate.

These two instances of failure in establishing stable mesothelial or mesothelioma clones expressing reporters that induce the production of autophagy regulators suggest that this cellular process plays a critical role in the survival mesothelial and mesothelioma cells and must be finely regulated. To overcome this issue, it could be useful to introduce the reporter in the cells via CRISPR/Cas9 method to have the reporter system expressed under the same promoter as the original gene (either *LC3* or *BCL2L1*, the gene encoding for BCL-X_L), instead of trying to integrate in the genome of the cells a reporter system that is expressed under a strong CMV promoter, as was attempted in this work.

I then developed another HTS approach for the study of MPM and decided to apply it to the field of drug resistance and tumour treatment. A collection of 1520 FDA-approved drugs was selected for

testing in this screening. Potential useful drugs for patient treatment revealed with such an approach would therefore need less testing and less time to proceed from the screening to approval for use in therapy. In this HTS approach, cell viability was used to evaluate the efficacy of drug combinations in killing mesothelioma cells. In particular, the killing effect of a collection of drugs administered alone or in combination with the chemotherapic agent cisplatin was assessed in NCI-H28 cells to identify drugs that work synergistically with cisplatin. In this instance, observing the effect exerted by the drugs alone is crucial to exclude from the possible hits all those drugs that were already toxic for mesothelioma cells on their own, and thus the effect seen when combined with cisplatin is not due to synergy. Moreover, toxicity of a drug alone may also indicate that drug is toxic for cells in general, not only mesothelioma cells. This could lead to the manifestation of adverse events in patients.

Different cell viability assays are commercially available for measuring cell viability, and they are mostly reliable, but these methods are usually based on the quantification of the levels of ATP (PerkinElmer ATPlite cat.# 6016943) or of some metabolic reaction (Sigma-Aldrich Resazurin assay cat.# R7017). These parameters could be influenced by some drugs without actually impacting the cell viability and the number of viable cells present in the well after treatment, so I decided to acquire images of the cells and use the count of the number of nuclei of live cells as the output reading for cell viability.

The selection of candidate drugs for use in therapy cannot rely solely on the results of the screening but must also be based on consideration regarding the availability of said drugs on the market, the available formulations of the drugs, their mechanisms of action and their side effects. So, even if some drugs may show an astounding activity *in vitro*, sometimes thy are still not the best choice for the treatment of a specific disease.

The HTS for drugs having a synergistic activity with cisplatin, followed by an accurate selection of the top screening hits, led to the choice of seven potentially effective drugs to be tested in further validation experiments: Riboflavin, Proglumide, Aminosalicylic acid, Gabapentin, Terfenadine, Propafenone, Oseltamivir.

Although the screening was performed three times, each time with a different final concentration of the screened drugs, testing them in such a small format as 384-well plates with only one well per screening condition leaves quite a chance for false positives to be detected. For this reason, it is important to test again the selected drugs in the same conditions as the screening, but in a bigger

format and with multiple replicates, to confirm the screening's results before proceeding with further tests. When the chosen drugs were tested again on NCI-H28 cells, four of the chosen drugs (Riboflavin, Proglumide, Aminosalicylic acid, and Gabapentin) were still effective in combination with cisplatin while being nontoxic alone, thus confirming what emerged from the screening, while Terfenadine, Propafenone, and Oseltamivir gave less convincing results. In particular, Terfenadine and Propafenone were found to be toxic for NCI-H28 cells when used alone at the highest concentrations, while Oseltamivir was simply not as effective as in the screening when combined with cisplatin.

Interestingly, while Riboflavin and Proglumide seemed to have a synergy with cisplatin at almost every tested concentration, Aminosalicylic acid and Gabapentin appeared to be more synergic at lower concentrations, while higher concentrations of these drugs took the levels of viable cells back to the ones displayed by cisplatin alone.

This effect could be explained by pharmacodynamics. Pharmacodynamics refers to the relationship between drug concentration at the site of action and the resulting effect, which is determined by that drug's binding with a receptor. The concentration at the site of the receptor usually determines the intensity its effect. However, other factors affect drug response, such as the receptor density on the cell surface, the mechanism of signal transmission through by second messengers, or the regulation of gene translation and protein production. The complex regulation of numerous cell processes may affect the way drugs interact with their target, making them more or less effective depending on the concentration of drug they have been exposed to.

Since different genetic alterations in mesothelioma can make this tumour susceptible to different drugs, I decided to test the chosen drugs on MSTO-211H, a cell line with a different genetic background than NCI-H28. In particular, MSTO-211H cells differ because, compared to NCI-H28, they lack a mutation in the *BAP1* gene [74]; [75]. This characteristic was chosen since loss of function *BAP1* mutations, such as the one carried by NCI-H28 cells, are known to have a role in chemoresistance to cisplatin [33]. This was supported also by my data showing a cisplatin EC_{50} of around 10µM for the *BAP1*-mutated NCI-H28 cells, while cisplatin EC_{50} was around 3µM for the *BAP1*-wild-type MSTO-211H cells. Interestingly, while results for Terfenadine, Propafenone and Oseltamivir were comparable to the ones obtained with NCI-H28 cells, the other drugs showed the same efficacy trend, but different efficacy levels, Gabapentin being the most effective synergic drug at all tested concentrations. This may indicate that these drugs work with different efficacy depending on the state of *BAP1* gene.

To measure the actual synergy with cisplatin, synergy tests were performed, and synergy score was given using dedicated algorithms (Lowe, Bliss, HAS). For all the drugs and tested in NCI-H28 cells, synergy was confirmed at the highest cisplatin concentration tested (20µM), but a high synergy score was obtained also at low cisplatin concentrations (0.6µM and/or 1.25µM) despite often not being significant. This could be due to the high standard deviation, since the results are based on only two replicates. The cisplatin concentrations in the middle did not show any synergy with the tested drugs, obtaining low scores.

These results are curious but can be explained by the cells responding differently to varying concentrations of cisplatin, for example expressing diverse receptors and modulating their expression differently, as well as modulating different metabolic pathways.

The same cannot be said about MSTO-211H cells, where different drugs had higher scores at different cisplatin concentrations. Riboflavin obtained the highest scores, despite not significant, at the tested concentration closest to cisplatin EC_{50} (2.5µM) for MSTO-211H cells, while Proglumide and Aminosalicylic acid obtained the higher, and significant, scores at higher concentrations (5µM and 10µM). Gabapentin obtained high and significant scores all throughout the tested cisplatin concentrations, except the lowest one (0.3µM). Strikingly, at this concentration Gabapenting was showing significant antagonism to cisplatin. Again, this effect it very curious, but could be explained by different concentrations of cisplatin inducing different changes in the treated cells.

Independently of cisplatin concentration and accordingly with the primary validation experiments, the drugs' concentrations obtaining higher synergy scores were the lowest ones, ranging from 0.3µM to 5µM, For NCI-H28 cells, while for MSTO-211H cells high scores were spread throughout all the tested concentrations.

To further evaluate the potential of the four selected drugs, they were tested on primary mesothelioma cells isolated from three different patients in combination with each patient's cell line's cisplatin EC_{50}. All the drugs were significantly synergistic in one of the patients' cells, but none of them was synergistic in the other two patients' cells, despite following the same trend as the other patient. This implies that different patients may have a different sensitivity to the tested drug combinations. It must be noted that the genetic background of these patients' tumours is still unknown, so assumptions cannot be made on the effect of genetic alterations on drug sensitivity in these patients. The state of *CDKN2A*, *BAP1*, and *NF2* in these patients will be verified to better understand their response to the tested drug combinations.

To better understand the mechanisms of action of these drugs, the expression of some markers of interest was analysed upon treatment with drugs in combination with cisplatin compared to cisplatin alone. The focus was centred on markers of chemoresistance (ABCB1, ABCG2), markers of cancer stem cells (CD24, OCT4), markers of senescence (p21), and regulation of autophagy and apoptosis (BCL-X_L). None of the drugs seemed to have a particular effect on the expression of any of these markers in NCI-H28 cells, suggesting that they may act through different cellular mechanisms. In MSTO-211H cells, Proglumide and Gabapentin, the two most effective drugs in the synergy tests, were significantly decreasing the expression of the cancer stem cell marker CD24, while Riboflavin and Aminosalicylic acid were producing only a slight and not significant decrease of CD24. This suggests that CD24-positive cancer stem cells in MSTO-211H may be very important for cancer cells' survival, but also targetable with drug combinations.

While these results are promising, we have to remember that the transcription levels of a protein may not match the actual protein levels in the cells. Thus, Western Blot analyses of these markers in both cell lines will be performed to confirm the RT-PCR data.

While two-dimensional studies of the selected drugs in mesothelioma cell lines may be promising, it must be kept in mind that the tumour environment in the patients is very different from the one of a tissue culture plate, starting from the tree-dimensional structure of the tumour. For this reason, I performed tests of the four selected drugs on mesothelioma spheroids. Unfortunately, treatment of the mesothelioma spheroids with combinations of drugs and cisplatin didn't produce any effect compared to treatment with cisplatin alone. This may be due to the drugs actually being unable to exert their effect in a 3D setting. In particular, given the high decrease in the sensitivity of organoids to cisplatin compared to 2D cultured mesothelioma cells (respectively 50µM vs 3µM to get 60% reduction in viability) we will increase accordingly the concentration of selected drugs in order to test a proportional range of concentrations.

In conclusion, despite the fact that many difficulties may arise during the design and application of HTS approaches, they remain a valuable tool for target and drug discovery in cancer studies. In this study, the use of HTS led to the discovery of four drugs that may improve the treatment of patients thanks to their synergy with the chemotherapeutic agent cisplatin. Of these four drugs, Proglumide is the one with the most consistent synergistic effect throughout the experiments and resulted especially powerful in the synergy score analysis. In addition to Proglumide, Riboflavin and Gabapentin should be considered for further testing, since their synergistic effect with cisplatin is

also pretty consistent, although less powerful than Proglumide. Furthermore, they would be perfect candidates for use in humans as combination therapies with cisplatin since Riboflavin (vitamin 2) and Gabapentin have already been proved to be safe to use together with this chemotherapeutic agent in animals and humans.

Although these results are very promising, it must be remembered that the genetic tumour background of each patient has an impact on the efficacy of therapies and must therefore be considered for choosing the proper treatment. Moreover, the study of drug efficiency in *in vitro* settings only is insufficient for the validation of drugs for use in human therapy. *In vivo* studies are also necessary to confirm drug safety and effectiveness and will be performed as a further validation step of the best drug candidates discovered with the present study.

8. References

1. Byrne, A.J., T.M. Maher, and C.M. Lloyd, *Pulmonary Macrophages: A New Therapeutic Pathway in Fibrosing Lung Disease?* Trends Mol Med, 2016. **22**(4): p. 303-316.
2. Bruno, R., et al., *Gene Expression Analysis of Biphasic Pleural Mesothelioma: New Potential Diagnostic and Prognostic Markers.* Diagnostics (Basel), 2022. **12**(3).
3. Refaeli, Y., et al., *Biochemical mechanisms of IL-2-regulated Fas-mediated T cell apoptosis.* Immunity, 1998. **8**(5): p. 615-23.
4. Beatty, G.L. and W.L. Gladney, *Immune escape mechanisms as a guide for cancer immunotherapy.* Clin Cancer Res, 2015. **21**(4): p. 687-92.
5. Bronte, G., et al., *The resistance related to targeted therapy in malignant pleural mesothelioma: Why has not the target been hit yet?* Crit Rev Oncol Hematol, 2016. **107**: p. 20-32.
6. Mossman, B.T. and A. Churg, *Mechanisms in the pathogenesis of asbestosis and silicosis.* Am J Respir Crit Care Med, 1998. **157**(5 Pt 1): p. 1666-80.
7. Warheit, D.B., et al., *Time course of chemotactic factor generation and the corresponding macrophage response to asbestos inhalation.* Am Rev Respir Dis, 1986. **134**(1): p. 128-33.
8. team, T.A.C.S.m.a.e.c., *Survival Rates for Malignant Mesothelioma.* American Cancer Society 2018.
9. Kazan-Allen, L. *International Ban Asbestos Secretariat*. 2022; 28 October 2022:[Available from: https://www.ibasecretariat.org/alpha_ban_list.php.
10. Hajj, G.N.M., et al., *Malignant pleural mesothelioma: an update.* J Bras Pneumol, 2021. **47**(6): p. e20210129.
11. Yilmaz, S., et al., *Effect of Asbestos Exposure on the Frequency of EGFR Mutations and ALK/ROS1 Rearrangements in Patients With Lung Adenocarcinoma: A Multicentric Study.* J Occup Environ Med, 2021. **63**(3): p. 238-243.
12. Ishida, T., et al., *Live-cell imaging of macrophage phagocytosis of asbestos fibers under fluorescence microscopy.* Genes Environ, 2019. **41**: p. 14.
13. Palomaki, J., et al., *Long, needle-like carbon nanotubes and asbestos activate the NLRP3 inflammasome through a similar mechanism.* ACS Nano, 2011. **5**(9): p. 6861-70.
14. Dostert, C., et al., *Innate immune activation through Nalp3 inflammasome sensing of asbestos and silica.* Science, 2008. **320**(5876): p. 674-7.
15. Xue, J., et al., *Asbestos induces mesothelial cell transformation via HMGB1-driven autophagy.* Proc Natl Acad Sci U S A, 2020. **117**(41): p. 25543-25552.
16. Filomeni, G., D. De Zio, and F. Cecconi, *Oxidative stress and autophagy: the clash between damage and metabolic needs.* Cell Death Differ, 2015. **22**(3): p. 377-88.
17. Dikic, I. and Z. Elazar, *Mechanism and medical implications of mammalian autophagy.* Nat Rev Mol Cell Biol, 2018. **19**(6): p. 349-364.

18. Levy, J.M.M., C.G. Towers, and A. Thorburn, *Targeting autophagy in cancer.* Nat Rev Cancer, 2017. **17**(9): p. 528-542.

19. Yu, L., Y. Chen, and S.A. Tooze, *Autophagy pathway: Cellular and molecular mechanisms.* Autophagy, 2018. **14**(2): p. 207-215.

20. Xu, D., et al., *Malignant pleural mesothelioma co-opts BCL-X(L) and autophagy to escape apoptosis.* Cell Death Dis, 2021. **12**(4): p. 406.

21. Avramescu, M.L., et al., *An investigation of the internal morphology of asbestos ferruginous bodies: constraining their role in the onset of malignant mesothelioma.* Part Fibre Toxicol, 2023. **20**(1): p. 19.

22. Alpert, N., M. van Gerwen, and E. Taioli, *Epidemiology of mesothelioma in the 21(st) century in Europe and the United States, 40 years after restricted/banned asbestos use.* Transl Lung Cancer Res, 2020. **9**(Suppl 1): p. S28-S38.

23. Chen, T., X.M. Sun, and L. Wu, *High Time for Complete Ban on Asbestos Use in Developing Countries.* JAMA Oncol, 2019. **5**(6): p. 779-780.

24. Popat, S., et al., *Malignant pleural mesothelioma: ESMO Clinical Practice Guidelines for diagnosis, treatment and follow-up(☆).* Ann Oncol, 2022. **33**(2): p. 129-142.

25. Barbieri, P.G., D. Consonni, and M. Schneider, *Accuracy of pleural biopsy for the diagnosis of histologic subtype of malignant pleural mesothelioma: Necropsy-based study of 134 cases.* Tumori, 2022. **108**(1): p. 26-32.

26. Ahmadzada, T., G. Reid, and S. Kao, *Biomarkers in malignant pleural mesothelioma: current status and future directions.* J Thorac Dis, 2018. **10**(Suppl 9): p. S1003-S1007.

27. Sauter, J.L., et al., *The 2021 WHO Classification of Tumors of the Pleura: Advances Since the 2015 Classification.* J Thorac Oncol, 2022. **17**(5): p. 608-622.

28. (NIH), N.C.I. *Cancer Staging* 2022 14 October 2022; Available from: https://www.cancer.gov/about-cancer/diagnosis-staging/staging.

29. Ruas, M. and G. Peters, *The p16INK4a/CDKN2A tumor suppressor and its relatives.* Biochim Biophys Acta, 1998. **1378**(2): p. F115-77.

30. Nag, S., et al., *The MDM2-p53 pathway revisited.* J Biomed Res, 2013. **27**(4): p. 254-71.

31. Franziska Kreidl , M.M., Eric Weitz , Finterly Hu , Egon Willighagen , Lauren J. Dupuis , Alex Pico , Lars Willighagen , and Kristina Hanspers. *WikiPathways Pleural mesothelioma (WP5087)* 2023 30 September 2023; Available from: https://www.wikipathways.org/pathways/WP5087.html.

32. LaFave, L.M., et al., *Loss of BAP1 function leads to EZH2-dependent transformation.* Nat Med, 2015. **21**(11): p. 1344-9.

33. Oehl, K., et al., *Alterations in BAP1 Are Associated with Cisplatin Resistance through Inhibition of Apoptosis in Malignant Pleural Mesothelioma.* Clin Cancer Res, 2021. **27**(8): p. 2277-2291.

34. Li, W., et al., *Merlin/NF2 loss-driven tumorigenesis linked to CRL4(DCAF1)-mediated inhibition of the hippo pathway kinases Lats1 and 2 in the nucleus.* Cancer Cell, 2014. **26**(1): p. 48-60.

35. Sato, T. and Y. Sekido, *NF2/Merlin Inactivation and Potential Therapeutic Targets in Mesothelioma.* Int J Mol Sci, 2018. **19**(4).

36. Yang, H., et al., *NF2 and Canonical Hippo-YAP Pathway Define Distinct Tumor Subsets Characterized by Different Immune Deficiency and Treatment Implications in Human Pleural Mesothelioma.* Cancers (Basel), 2021. **13**(7).

37. Ou, S.H., et al., *SWOG S0722: phase II study of mTOR inhibitor everolimus (RAD001) in advanced malignant pleural mesothelioma (MPM).* J Thorac Oncol, 2015. **10**(2): p. 387-91.

38. Zauderer, M.G., et al., *Phase 1 cohort expansion study of LY3023414, a dual PI3K/mTOR inhibitor, in patients with advanced mesothelioma.* Invest New Drugs, 2021. **39**(4): p. 1081-1088.

39. Cakiroglu, E. and S. Senturk, *Genomics and Functional Genomics of Malignant Pleural Mesothelioma.* Int J Mol Sci, 2020. **21**(17).

40. Browne, S. and M. Lechat, *Albert Dubois, M.D., D.T.M. 1888-1977.* Int J Lepr Other Mycobact Dis, 1978. **46**(1): p. 69.

41. Vlahu, T. and W.T. Vigneswaran, *Pleurectomy and decortication.* Ann Transl Med, 2017. **5**(11): p. 246.

42. Duranti, L., et al., *Extra-pleural pneumonectomy.* J Thorac Dis, 2019. **11**(3): p. 1022-1030.

43. Flores, R.M., *Surgical options in malignant pleural mesothelioma: extrapleural pneumonectomy or pleurectomy/decortication.* Semin Thorac Cardiovasc Surg, 2009. **21**(2): p. 149-53.

44. Dasari, S. and P.B. Tchounwou, *Cisplatin in cancer therapy: molecular mechanisms of action.* Eur J Pharmacol, 2014. **740**: p. 364-78.

45. Vogelzang, N.J., et al., *Phase III study of pemetrexed in combination with cisplatin versus cisplatin alone in patients with malignant pleural mesothelioma.* J Clin Oncol, 2003. **21**(14): p. 2636-44.

46. Fossella, F.V. and U. Gatzemeier, *Phase I trials of pemetrexed.* Semin Oncol, 2002. **29**(2 Suppl 5): p. 8-16.

47. Yang, T.Y., et al., *Effect of folic acid and vitamin B12 on pemetrexed antifolate chemotherapy in nutrient lung cancer cells.* Biomed Res Int, 2013. **2013**: p. 389046.

48. Cinausero, M., et al., *Chemotherapy treatment in malignant pleural mesothelioma: a difficult history.* J Thorac Dis, 2018. **10**(Suppl 2): p. S304-S310.

49. Zalcman, G., et al., *Bevacizumab for newly diagnosed pleural mesothelioma in the Mesothelioma Avastin Cisplatin Pemetrexed Study (MAPS): a randomised, controlled, open-label, phase 3 trial.* Lancet, 2016. **387**(10026): p. 1405-1414.

50. Gomez, D.R., et al., *The Use of Radiation Therapy for the Treatment of Malignant Pleural Mesothelioma: Expert Opinion from the National Cancer Institute Thoracic Malignancy Steering Committee, International Association for the Study of Lung Cancer, and Mesothelioma Applied Research Foundation.* J Thorac Oncol, 2019. **14**(7): p. 1172-1183.

51. Cho, B.C., et al., *A feasibility study evaluating Surgery for Mesothelioma After Radiation Therapy: the "SMART" approach for resectable malignant pleural mesothelioma.* J Thorac Oncol, 2014. **9**(3): p. 397-402.

52. Chen, L., *Co-inhibitory molecules of the B7-CD28 family in the control of T-cell immunity.* Nat Rev Immunol, 2004. **4**(5): p. 336-47.

53. *[In memory of Robert Bauer, Dec 11, 1898--Mar 31, 1975].* Z Allgemeinmed, 1975. **51**(20): p. 923.

54. Shephard, D.A., *Editorial: The metric system, the International System of Unist (SI) and medicine.* Can Med Assoc J, 1975. **112**(7): p. 799-801.

55. Brcic, L., et al., *Prognostic impact of PD-1 and PD-L1 expression in malignant pleural mesothelioma: an international multicenter study.* Transl Lung Cancer Res, 2021. **10**(4): p. 1594-1607.

56. Brahmer, J.R., et al., *Phase I study of single-agent anti-programmed death-1 (MDX-1106) in refractory solid tumors: safety, clinical activity, pharmacodynamics, and immunologic correlates.* J Clin Oncol, 2010. **28**(19): p. 3167-75.

57. Aliagas, E., et al., *Efficacy of CDK4/6 inhibitors in preclinical models of malignant pleural mesothelioma.* Br J Cancer, 2021. **125**(10): p. 1365-1376.

58. Fennell, D.A., et al., *Abemaciclib in patients with p16ink4A-deficient mesothelioma (MiST2): a single-arm, open-label, phase 2 trial.* Lancet Oncol, 2022. **23**(3): p. 374-381.

59. Roe, O.D., et al., *Malignant pleural mesothelioma: genome-wide expression patterns reflecting general resistance mechanisms and a proposal of novel targets.* Lung Cancer, 2010. **67**(1): p. 57-68.

60. Zhang, S. and Y. Wang, *Deoxyshikonin inhibits cisplatin resistance of non-small-cell lung cancer cells by repressing Akt-mediated ABCB1 expression and function.* J Biochem Mol Toxicol, 2020. **34**(10): p. e22560.

61. Hu, C.F., et al., *Upregulation of ABCG2 via the PI3K-Akt pathway contributes to acidic microenvironment-induced cisplatin resistance in A549 and LTEP-a-2 lung cancer cells.* Oncol Rep, 2016. **36**(1): p. 455-61.

62. Ghani, F.I., et al., *Identification of cancer stem cell markers in human malignant mesothelioma cells.* Biochem Biophys Res Commun, 2011. **404**(2): p. 735-42.

63. Blum, W., et al., *Stem Cell Factor-Based Identification and Functional Properties of In Vitro-Selected Subpopulations of Malignant Mesothelioma Cells.* Stem Cell Reports, 2017. **8**(4): p. 1005-1017.

64. Al-Madhagi, H.A., *FDA-approved drugs in 2022: A brief outline.* Saudi Pharm J, 2023. **31**(3): p. 401-409.

65. Close, D.A., et al., *Unbiased High-Throughput Drug Combination Pilot Screening Identifies Synergistic Drug Combinations Effective against Patient-Derived and Drug-Resistant Melanoma Cell Lines.* SLAS Discov, 2021. **26**(5): p. 712-729.

66. Nair, N.U., et al., *A landscape of response to drug combinations in non-small cell lung cancer.* Nat Commun, 2023. **14**(1): p. 3830.

67. Xie, J., C. Wang, and J.C. Gore, *High Throughput Screening for Colorectal Cancer Specific Compounds.* Comb Chem High Throughput Screen, 2016. **19**(3): p. 180-8.

68. Dell'Anno, I., et al., *A Drug Screening Revealed Novel Potential Agents against Malignant Pleural Mesothelioma.* Cancers (Basel), 2022. **14**(10).

69. A. Laure, A.R., M. Manovah, M. Chambon, G. Turcatti, M. Kirschner, I. Opitz, S. Hiltbrunner, A. Curioni-Fontecedro, *137P Repurposing drug screen of patient-derived malignant pleural mesothelioma cells reveals potential anti-cancer activity.* Journal of Thoracic Oncology, 2023. **18**(4): p. S117-S118.

70. Akiyama, T., J. Selhub, and I.H. Rosenberg, *FMN phosphatase and FAD pyrophosphatase in rat intestinal brush borders: role in intestinal absorption of dietary riboflavin.* J Nutr, 1982. **112**(2): p. 263-8.

71. Beauchamp, R.D., et al., *Proglumide, a gastrin receptor antagonist, inhibits growth of colon cancer and enhances survival in mice.* Ann Surg, 1985. **202**(3): p. 303-9.

72. Glanz, V.Y., et al., *Inhibition of sialidase activity as a therapeutic approach.* Drug Des Devel Ther, 2018. **12**: p. 3431-3437.

73. Usami, N., et al., *Establishment and characterization of four malignant pleural mesothelioma cell lines from Japanese patients.* Cancer Sci, 2006. **97**(5): p. 387-94.

74. Yoshikawa, Y., et al., *Frequent inactivation of the BAP1 gene in epithelioid-type malignant mesothelioma.* Cancer Sci, 2012. **103**(5): p. 868-74.

75. Bott, M., et al., *The nuclear deubiquitinase BAP1 is commonly inactivated by somatic mutations and 3p21.1 losses in malignant pleural mesothelioma.* Nat Genet, 2011. **43**(7): p. 668-72.

76. Bodiga, V.L., et al., *Effect of vitamin supplementation on cisplatin-induced intestinal epithelial cell apoptosis in Wistar/NIN rats.* Nutrition, 2012. **28**(5): p. 572-80.

77. Hassan, I., S. Chibber, and I. Naseem, *Vitamin B(2): a promising adjuvant in cisplatin based chemoradiotherapy by cellular redox management.* Food Chem Toxicol, 2013. **59**: p. 715-23.

78. Tsavaris, N., et al., *Gabapentin monotherapy for the treatment of chemotherapy-induced neuropathic pain: a pilot study.* Pain Med, 2008. **9**(8): p. 1209-16.

79. Warnier, M., et al., *CACNA2D2 promotes tumorigenesis by stimulating cell proliferation and angiogenesis.* Oncogene, 2015. **34**(42): p. 5383-94.